

For reprint orders, please contact: reprints@future-science.com

Discovery of new chemotypes of dual 5-HT_{2A}/D₂ receptor antagonists with a strategy of drug design methodologies

Milica Radan^{*,1,2} , Teodora Djikic¹  & Katarina Nikolic^{**,1} 

¹University of Belgrade, Faculty of Pharmacy, Department of Pharmaceutical Chemistry, Vojvode Stepe 450, Belgrade, 11000, Serbia

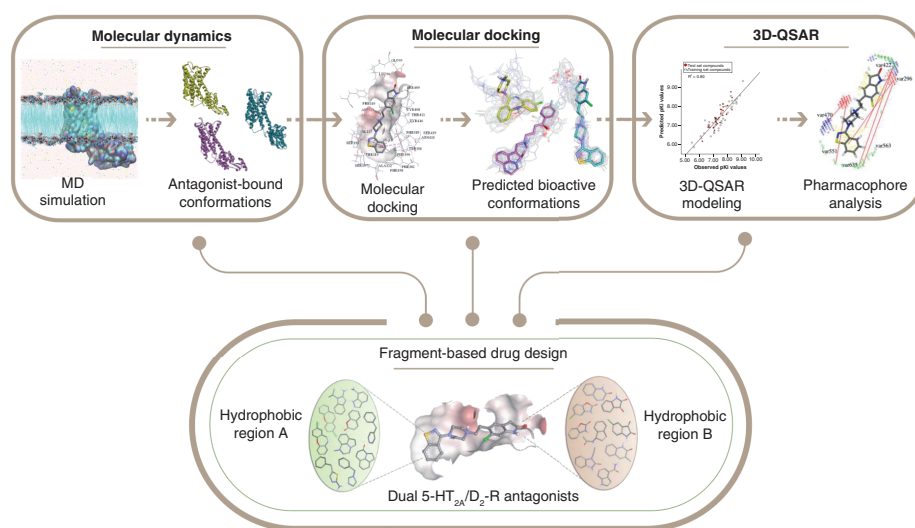
²Institute for Medicinal Plant Research Dr. Josif Pančić, Tadeuša Koščuška 1, Belgrade, 11000, Serbia

*Author for correspondence: milica.r994@live.com

**Author for correspondence: knikolic@pharmacy.bg.ac.rs

Aim: Through the application of structure- and ligand-based methods, the authors aimed to create an integrative approach to developing a computational protocol for the rational drug design of potent dual 5-HT_{2A}/D₂ receptor antagonists without off-target activities on H₁ receptors. **Materials & methods:** Molecular dynamics and virtual docking methods were used to identify key interactions of the structurally diverse antagonists in the binding sites of the studied targets, and to generate their bioactive conformations for further 3D-quantitative structure–activity relationship modeling. **Results & conclusion:** Toward the goal of finding multi-potent drugs with a more effective and safer profile, the obtained results led to the design of a new set of dual antagonists and opened a new perspective on the therapy for complex brain diseases.

Graphical abstract:



First draft submitted: 12 December 2021; Accepted for publication: 26 April 2022; Published online: 8 June 2022

Keywords: 3D-QSAR • 5-HT_{2A} • D₂ • fragment-based drug design • H₁ • molecular docking • molecular dynamics simulations

Neurological and mental disorders are the leading causes of disability and impairment of quality of life in the world. Globally, it is estimated that they affect 13% of the population, while around 40% of the European Union population suffers from at least one disease from the neuropsychiatric spectrum [1–4]. Moreover, the COVID-

19 pandemic has significantly affected the mental health of people worldwide [5]. Even though the overall impact on mental well-being is not yet clear, it is possible to conclude that these disorders are an international public health priority with marked consequences for society [6].

Neurological diseases are very often associated with mental disorders and both are characterized by an imbalance of neurotransmitter systems in the brain. The serotonergic and dopaminergic systems appear to be involved in the regulation of not only motor but also non-motor functions, such as cognition, mood, behavior and neuroendocrine secretion [7,8]. Nevertheless, the dysfunction of dopamine (DA) and 5-hydroxytryptamine, 5-HT (serotonin) neurotransmission in the central nervous system (CNS) has been involved in the pathogenesis of various brain disorders, such as anxiety, depression, schizophrenia and Parkinson's disease [8–13].

In fact, the balanced modulation of serotonin 5-HT_{2A} receptor (5-HT_{2A}-R) and dopamine D₂ receptor (D₂-R) is crucial for the effective treatment of these multi-factorial brain disorders [14]. Antagonism of these receptors presents a main mechanism of action for the antipsychotic efficacy of the second-generation atypical antipsychotics (AAPs) [15]. Compared with typical antipsychotics (TAPs), which are known to be potent D₂-R antagonists, AAPs are considered multi-target directed compounds [15,16]. Many studies have shown that AAPs, despite being able to control a variety of the positive symptoms of psychosis, are also very effective in alleviating the negative symptoms as well as cognitive dysfunction [15–18]. Moreover, they are less likely to cause the adverse effects associated with motor activity and extrapyramidal symptoms (EPSs) [19]. Although a multi-target approach tends to be beneficial, its polypharmacological profile may increase the occurrence of side effects. Off-target activity on the histamine H₁ receptors (H₁-Rs) has been reported to be highly correlated with metabolic dysregulation caused by antipsychotics [20–22].

Utilization of computer-aided drug design (CADD) methods in the process of rational drug design has an important role in the discovery of new compounds with an optimal polypharmacological profile [23,24]. Establishing balanced modulation of these targets is very challenging but could be effectively examined through the integration of different drug design methods, which are commonly divided into ligand-based drug design (LBDD) and structure-based drug design (SBDD) methods [25]. 3D-quantitative structure–activity relationship (3D-QSAR) represents one of the most frequently used LBDD approaches to pharmacophore analysis and activity prediction of newly designed compounds [24,26]. On the other hand, SBDD approaches, such as molecular dynamics (MD) simulations and molecular docking, aim to simulate the dynamic behavior of molecular systems and to predict the best binding mode of a studied ligand to a protein [27,28]. Since crystal structures of 5-HT_{2A}-Rs, D₂-Rs and H₁-Rs are available [29–31], the integration of such approaches may be a beneficial strategy to obtain more reliable results for the design of potential novel therapeutics.

Therefore, the design of multi-functional compounds with optimal antagonistic activity on both 5-HT_{2A}-Rs and D₂-Rs, and with a lower binding affinity to the H₁-Rs, may present a significant advance in the treatment of neuropsychiatric disorders. Even though there are many approved drugs on the market, there is still a great need to develop medications with good efficacy and an improved safety profile. Unlike previous studies, this one was based on a comprehensive pharmacophore analysis of dual 5-HT_{2A}/D₂ receptor (5-HT_{2A}/D₂-R) antagonists, taking into account their selectivity against H₁-Rs [32–35]. Particularly, datasets consisting of chemical structures with a wide range of experimental activity and structural diversity were employed for the careful analysis of key interactions in proteins' binding sites utilizing MD and molecular docking methods. This study also included derivatives of lumateperone, which is a potent dual 5-HT_{2A}/D₂-R antagonist recently approved for the treatment of schizophrenia in adults [36]. Furthermore, the specific bioactive conformations of the tested compounds were used to elucidate which molecular determinants influence the 5-HT_{2A}/D₂-R antagonistic activity and selectivity against the H₁-R. This way, the authors obtain more realistic and trustworthy results regarding how structurally different compounds bind and modulate the activity of the studied receptors, providing valuable information for the design of novel antagonists with a desired activity profile.

Materials & methods

Dataset preparation

In this study, a broad spectrum of structurally diverse antagonists were used for pharmacophore analysis and 3D-QSAR model building. The principal component analysis (PCA) was employed in Pentacle [37] to inspect the structural similarities of the studied compounds based on the calculated grid independent descriptors (GRINDs) [38]. Following the obtained findings (Supplementary Figure 1), dataset compounds could be divided into three different clusters, including cluster one – tricyclic derivatives of dibenzocycloheptene (clozapine-like compounds), cluster

two – derivatives of 1,2-benzisothiazole (ziprasidone-like compounds) and cluster three – tetracyclic quinoxaline derivatives (lumateperone-like compounds).

Clozapine, ziprasidone and lumateperone belong to a group of atypical antipsychotics that are known to be potent 5-HT_{2A}/D₂-R antagonists. Due to their well-known efficacy in treating patients experiencing psychotic symptoms, they represent great lead molecules for further investigations. Moreover, ziprasidone and lumateperone were found to have a lower tendency to induce metabolic side effects compared with clozapine [39,40]. Therefore, these compounds were chosen to be cluster representatives in order to elucidate key structural features important for the activation of target proteins.

Namely, the datasets for 5-HT_{2A}-R and D₂-R comprised cluster one (Supplementary Figures 2 & 3), cluster two (Supplementary Figure 4) and cluster three (Supplementary Figure 5) compounds [22,41–44]. On the other hand, the dataset for H₁-R included compounds from cluster one and cluster two only [41,45]. However, lumateperone-like derivatives from cluster three were not included in the 3D-QSAR study for H₁-R due to the absence of experimental data.

All examined compounds were downloaded from the ChEMBL database (www.ebi.ac.uk/chembl/) with their antagonistic activities expressed as negative logarithm of inhibition constant (pKi=-logKi) (Supplementary Tables 1–3). The pKi distribution range for 5-HT_{2A}-R was 5.92–11.00, while slightly lower values were observed for the D₂-R model, 5.52–9.05, as well as for H₁-R, 5.06–9.86. Since wide ranges of activity values are preferable in building regression models, the use of selected datasets will ensure their good predictive power and wide applicability. The MarvinSketch program [46] was used for the selection of dominant forms of compounds at physiological pH 7.4. Furthermore, selected forms were submitted for energy minimization by the semi-empirical Parameterized Model revision 3 (PM3) method [47,48] and Hartree-Fock/3-21G method [49] from Gaussian software [50] included in Chem3D Ultra (Chem3D Ultra v7.0, 2001, www.cambridgesoft.com/) [51]. The final ligand's conformations were selected after employing MD and molecular docking studies.

MD simulation

MD as an SBDD method requires 3D protein structure to provide deeper insight into the protein–ligand interactions and binding conformations. 5-HT_{2A}-Rs, D₂-Rs and H₁-Rs belong to the rhodopsin-like family of G protein-coupled receptors (GPCRs). They consist of seven transmembrane (TM) helices, three intracellular loops (ICLs) and three extracellular loops (ECLs), which were also found to play a critical role in ligand binding specificity. Previously reported crystallographic studies on target receptors revealed their high-resolution crystal structures in inactive conformations. Both, 5-HT₂-R and D₂-R were determined in complexes with widely known atypical antipsychotic risperidone at 3.0 Å and 2.9 Å resolutions, respectively (PDB ID: 6a93, 6 cm4), whereas H₁-R was purified in complex with a first-generation antagonist, doxepin at a resolution of 3.1 Å (PDB ID: 3rze) [29–31]. Selected crystal structures were downloaded from the Protein Data Bank (PDB) database [52].

The PlayMolecule web platform was used for the protonation of examined proteins at physiological pH 7.4 [53]. Cluster reference ligands were docked into protein 3D structures using AutoDock Vina (AD Vina) software [54,55]. Actually, three separate simulations were performed for each studied receptor in complexes with clozapine (ChEMBL42), ziprasidone (ChEMBL708) and lumateperone (ChEMBL3233142). The α carbon coordinates of Asp^{3×32} (Asp155 for 5-HT_{2A}-R, Asp114 for D₂-R and Asp107 for H₁-R) were used for grid centering in all cases and the grid box was set to be 12 Å, enabling ligand to rotate freely in the binding pocket.

As in some previous studies on GPCRs, 50 ns of production phase was executed on the system to ensure that simulations lasted long enough to reach an equilibrium [56–58]. The Visual Molecular Dynamics (VMD) program [59] was used to prepare the system, while Nanoscale Molecular Dynamics (NAMD) was utilized for MD simulations [60]. Since the studied proteins belong to GPCRs, the membrane environment was simulated with 1,2-palmitoyl-oleoyln-glycero-3-phosphocholine (POPC) membrane (membrane dimensions of X and Y were set to 80 Å in the case of 5-HT_{2A}-R and 120 Å in the case of D₂-R and H₁-R). The CHARMM General Force Field (CGenFF) web platform was used to generate the ligands' topology files [61,62]. The CHARMM36 force field for lipids and proteins were applied to enable the hybrid system. The TIP3P water model was used for solvation of the whole system, while neutralization was performed with NaCl at 0.2 M concentration. Distance cutoff for Van der Waals (VdW) and electrostatic calculations was set to 12 Å. Generally, the entire simulation process could be divided into several steps: minimization, equilibration and production run. The initial minimization was performed with flexible lipid tails, and all other atoms fixed (protein, ligand, water, ions and lipid head groups). After 1000 steps of minimization, the velocities were reinitiated to the desired temperature, and equilibration was run for

0.5 ns (using a 2 fs timestep). The second minimization run was performed with harmonic constraints imposed on the protein, which enabled lipids, ions and water to adapt to the receptor. The minimization was then followed by an equilibration to prevent hydration of the hydrophobic regions. Subsequently, the whole system was further equilibrated without any constraints. Finally, the production run for each simulation was carried out for 50 ns at a temperature of 310 K and pressure of 1 atm. Fluctuations in the barostat were controlled with Langevin dynamics (Nose–Hoover method). The root mean square deviation (RMSD), solvent accessible surface area (SASA) and number of hydrogen bond values were used to verify the stability of the performed simulations and were measured by VMD.

Molecular docking

Molecular docking is a frequently used CADD technique for the analysis of binding site interactions as well as free energy of binding calculation [63]. Starting from the obtained antagonist-bound conformations from MD simulations, the authors aimed to predict the predominant bioactive conformers of all examined ligands by using AD Vina software [55].

Namely, nine different complexes were subjected to MD study (5-HT_{2A}-R–clozapine, 5-HT_{2A}-R–ziprasidone, 5-HT_{2A}-R–lumateperone, D₂-R–clozapine, D₂-R–ziprasidone, D₂-R–lumateperone, H₁-R–clozapine, H₁-R–ziprasidone and H₁-R–lumateperone). The last frame of each simulation was extracted and used in molecular docking analysis. The obtained inactive conformations of studied targets in complexes with reference ligands were further employed as templates for conformer generation. Therefore, dataset ligands were docked into the appropriate receptor conformation depending on which cluster they belong to. Precisely, ligands from cluster one were docked into the receptor's conformation after simulation with clozapine and ligands from cluster two after simulation with ziprasidone, while ligands from cluster three were docked into the receptor's conformation after simulation with lumateperone. Flexible ligand sampling was used as a docking procedure in AD Vina, while the protein conformation was considered to be fixed. The grid box size was set to 12 Å for each direction, while the coordinates of the α carbon of asparagine amino acid (Asp155-5-HT_{2A}-R, Asp114-D₂-R and Asp107-H₁-R) were used as grid center. The conformations were explored with pose generation set to 20 and exhaustiveness value set to 50. Based on the binding mode similarity to a reference ligand, as well as AD Vina docking score, the final ligands' conformations were selected and utilized for further 3D-QSAR analysis. All docked complexes were visualized and illustrated using Discovery Studio Visualizer [64].

3D-QSAR modeling

The Pentacle program [37] was utilized for 3D-QSAR analysis in order to identify molecular determinants that influence the antagonistic activity of the studied compounds at 5-HT_{2A}-Rs, D₂-Rs and H₁-Rs. It is based on the calculation of GRINDs (GRIND and GRIND2) [65]. They represent 3D-based molecular descriptors that are obtained from molecular interaction fields (MIFs). Four different chemical probes, with 0.5 Å grid step, were used to compute MIFs, including the TIP probe, which represents the shape of the molecule; the DRY probe, which designates hydrophobic interactions; the N1 probe, which denotes hydrogen bond donor (HBD) groups; and the O probe, which represents hydrogen bond acceptor (HBA) groups. Starting from the different types of grid-computed MIFs, the discretization algorithm ALMOND was used to extract the highly relevant regions (hot spots) that could contribute to the binding affinity. The number of nodes was set to 100, while the weight was set to 50%. To encode the filtered MIFs into GRIND variables, the authors employed the consistently large auto and cross correlation (CLACC) algorithm, with a 0.8 smoothing window [66]. Finally, the obtained results were presented as correlograms where each variable was defined as the interaction of two grid nodes, which belong to certain MIF types, at a specific distance range. The large number of initially calculated descriptors was reduced using fractional factorial design (FFD) generating optimal linear partial least squares (PLS) estimations (GOLPEs) in order to obtain the most significant GRIND variables [67]. Afterward, PLS regression analysis was used for 3D-QSAR model building.

Based on the PCA score plot and the common structural features, the whole datasets of 5-HT_{2A}-R (n = 80), D₂-R (n = 73) and H₁-R (n = 48) were divided into training (70%) and test (30%) set compounds. In fact, the test set was selected such that each compound remained close to at least one of the training set compounds from the same cluster, taking into account that the pK_i values were homogeneously distributed throughout the range. The training set comprised the rest of the compounds, providing a wide range of experimental activities and structural diversity for model building. The 3D-QSAR model for 5-HT_{2A}-R contained 54 and 26 compounds (Supplementary Table

1), the model for D₂-R consisted of 49 and 24 compounds (Supplementary Table 2) and the H₁-R 3D-QSAR model contained 32 and 16 compounds in the training and test sets, respectively (Supplementary Table 3).

3D-QSAR model validation

The created 3D-QSAR models were evaluated by applying the internal and external validation procedure with the aim to confirm their reliability and predictability. In quantitative activity prediction, statistical parameters, including predicted residual sum of squares (PRESS), cross-validated squared correlation coefficient (Q²) and root mean square error of estimation (RMSEE), are widely used as statistical metrics of internal model predictability and robustness [68]. They were calculated by Equations 1–3 considering compounds from the training set only.

$$PRESS = \sum_{i=1}^n e_{(i)}^2 \quad (\text{Equation 1})$$

$$Q^2 = 1 - \frac{PRESS}{\sum (Y_{obs(training)} - \bar{Y}_{obs(training)})^2} \quad (\text{Equation 2})$$

$$RMSEE = \sqrt{\frac{PRESS}{n}} \quad (\text{Equation 3})$$

The $e_{(i)}$ corresponds to the difference between the observed and predicted Y values, whereas n defines the number of compounds in the training set. Observed (experimental) pKi value for the training set compounds is denoted by $Y_{obs(training)}$, while $\bar{Y}_{training}$ represents the average pKi value. Models with good predictive power should have Q² value higher than 0.50, while RMSEE value should be as small as possible [68–70].

Although the high value of Q² is very important for model validation, it is not a sufficient parameter to describe the predictive potential of the created 3D-QSAR model for the new dataset [69,71]. For that reason, it is necessary to perform model validation by using the external, test set, molecules. In order to assess the external capability of the created models, parameters such as determination coefficient (R^2_{pred}) and root mean square error of prediction (RMSEP), defined in Equation 4 and Equation 5, respectively, were calculated.

$$R^2_{pred} = 1 - \frac{PRESS}{\sum (Y_{obs(test)} - \bar{Y}_{obs(training)})^2} \quad (\text{Equation 4})$$

$$RMSEP = \sqrt{\frac{PRESS}{n}} \quad (\text{Equation 5})$$

The parameter $Y_{obs(test)}$ corresponds to an observed pKi value of the molecules from the test set, while $\bar{Y}_{training}$ represents an average pKi value calculated for the compounds from the training set. In Equation 5, n represents the number of test set compounds. 3D-QSAR models with high predictive power should have R^2_{pred} higher than 0.50 and a low value of RMSEP (≤ 2 RMSEE) [68,70,71].

Moreover, for deeper analysis of the created models, the authors applied $r^2_{metrics}$ (r^2_m , r'^2_m , r^{*2}_m and Δr^2_m) validation [68,72]. These statistical parameters are not dependent on the $\bar{Y}_{training}$ value, enabling them to more precisely describe the external predictability of the created 3D-QSAR models. The following parameters, r^2_m and r'^2_m , were calculated by Equation 6 and Equation 7:

$$r^2_m = r^2(1 - \sqrt{|r^2 - r_0^2|}) \quad (\text{Equation 6})$$

$$r'^2_m = r^2(1 - \sqrt{|r^2 - r_0'^2|}) \quad (\text{Equation 7})$$

where r represents the correlation between observed and predicted pKi values, while the intercept r_0 was obtained by interchanging the axes. The values of r^2_m , r'^2_m as well as their average value (r^{*2}_m) should be close and greater than 0.50, while the absolute difference between r^2_m and r'^2_m (Δr^2_m) should be lower than 0.20 for an acceptable model [68,71,73].

Applicability domain

Establishment of the applicability domain (AD) is one of the five principles proposed by the Organization for Economic Cooperation and Development (OECD) and should be followed in the process of building reliable and acceptable 3D-QSAR models [74]. It actually represents the chemical structure space defined with the properties of the training set compounds [75]. The activity prediction of new compounds might be considered accurate only if it falls within the defined AD of the created 3D-QSAR model. For the present work, the authors employed the leverage approach (Williams plot) using SPSS software [76,77]. The warning leverage value (h^*) was calculated by Equation 8.

$$h^* = 3(p + 1)/n \quad (\text{Equation 8})$$

The number of the model variables is represented by p , while n denotes the number of compounds in the training set (Equation 10). If the calculated leverage value of a molecule is higher than the warning value (h^*), the prediction is not completely reliable, since the compound is outside the defined AD.

Fragment-based drug design

The fragment-based drug design (FBDD) method was employed in order to rationally design novel potent antagonists with the desired target profile. It presents an attractive approach for rapid and efficient screening of the fragment libraries, offering good starting points for designing novel compounds [78]. In particular, two commercially available fragment libraries, the General Fragment Library and Enamine Essential Fragment Library, were used to find the most suitable building blocks to act as lead skeletons for developing high-affinity ligands against protein targets. The General Fragment Library was selected due to the largest number of fragments among others available from Life Chemicals, Inc. It contained nearly 51,000 fragment-like molecules that were filtered on molecular weight (MW) ≤ 300 as well as lipophilicity expressed as the calculated octanol/water partition coefficient (ClogP) ≤ 3.0 . Moreover, the Enamine Essential Fragment Library obtained from Enamine Ltd was added with the aim to further expand the chemical diversity of the final fragment library. It comprised of 320 fragments with MW < 250 , number of HBAs/HBDs < 3 , ClogP < 2.5 and topological polar surface area (TPSA) $< 60 \text{ \AA}$. Structural moieties of ChEMBL90882 and ziprasidone were used as templates for fragment-based screening of the previously mentioned databases by the Fingerprints for Ligands and Proteins (FLAP) program v2.2 [79,80]. Selected compounds exhibited high affinities for both 5-HT_{2A}-Rs and D₂-Rs and were found to interact with the key pocket residues, therefore representing good starting points for further rational drug design.

First, the General Fragment Library was pre-filtered to reduce the size of the dataset. All fragments from the library were inspected in terms of shape similarity to the selected templates, 1,2-benzothiazol and 1,3-dihydro-2-oxindol from ziprasidone and dibenzoxepin from ChEMBL90882. Subsequently, fragments with the best Glob-Sum similarity scores (which represent the sum of scores from grid probes), were chosen to build a new database for more precise screening. The final created database contained pre-filtered fragments of the General Fragment Library and Enamine database fragments. For each molecule (fragments from library and templates), grid MIFs were calculated using four probes representing the most important interaction types, such as HBA and HBD, hydrophobic and shape [81]. After determining energetically favorable interactions, MIFs were condensed into four pharmacophoric points, termed quadruplets. FLAP was further utilized to align the fragments from the database to the selected templates and to discover the best overlap by comparing the quadruplets. Basically, the FLAP similarity represents the Tanimoto similarity between the candidate MIF and the template MIF. It is based on the assumption that fragments with higher similarity are more likely to bind to the receptor in the same manner. The Glob-Sum similarity score was used to select the best aligned fragments for subsequent rational drug design of novel compounds by the fragment-linking approach [78].

In silico absorption, distribution, metabolism, excretion & toxicity profiling

In silico prediction of the absorption, distribution, metabolism, excretion and toxicity (ADMET) properties of compounds is one of the most significant steps in the process of rational drug design [82]. In this study, the results obtained from ADMET Predictor software [83] were assembled and used for a description of the physico-chemical and pharmacokinetic properties of all the designed antagonists, along with lead molecules. The best candidates with an optimal pharmacokinetic profile, synthetic tractability and predicted *in silico* activity were chosen for further optimization.

Results & discussion

In recent times, a polypharmacological strategy for the treatment of complex neurological and mental diseases has been proposed as a key concept in the development of novel CNS drug candidates that act on multiple targets simultaneously [84]. Herein, the authors describe a pharmacophore of dual 5-HT_{2A}/D₂-R antagonists, taking into account their H₁-R activity by employing different CADD approaches.

MD & molecular docking

In the current study, nine different MD simulations of the studied targets in complexes with reference ligands were performed. 5-HT_{2A}-Rs, D₂-Rs and H₁-Rs represent membrane-embedded proteins, which belong to the GPCR family. It has been found that membrane lipids have a significant stabilization effect on protein conformational states in MD simulations [85]. Furthermore, different analytical tools were used to investigate the quality of the performed MD simulations as well as to ensure that they lasted long enough to reach equilibrium.

The RMSD is one of the most frequently used analyses for revealing the conformational changes and structure stability of a protein. It calculates the distance between atomic coordinates in the trajectory. Lower deviations (usually, <2 Å) indicate that there are no significant conformational changes in the system, which could be considered equilibrated [86]. In accordance with the aim to assess the stability of studied complexes during the simulation time, RMSD plots for the receptor backbone, ligand and residues in the binding site were generated (Supplementary Figures 6–8). From the obtained results, the authors concluded that receptor backbone RMSD values for all complexes remained steady after approximately 25 ns, and some even before. After 15 ns, the backbone RMSD values of 5-HT_{2A}-R and D₂-R in complexes with clozapine (Supplementary Figures 6B & 7B) kept stable around 1.2 Å and 1.6 Å, respectively. The RMSD values for the 5-HT_{2A}-R–ziprasidone and D₂-R–ziprasidone complexes (Supplementary Figures 6F & 7F) remained stabilized around 1 Å and 1.4 Å after 25 ns, while the values of the 5-HT_{2A}-R–lumateperone and D₂-R–lumateperone complexes (Supplementary Figures 6J & 7J) slightly floated around 1.4 Å and 1 Å, respectively. Moreover, it can be observed that the backbone RMSD values for clozapine and ziprasidone complexes with H₁-R (Supplementary Figure 8B & F) were stabilized around 1.5 Å and for lumateperone around 1.2 Å (Supplementary Figure 8J) after approximately 5 ns, indicating that these complexes were also stable. Ligand RMSD fluctuations less than 1 Å in all complexes indicated that the simulated compound was stabilized in the receptor binding pocket in its most favorable conformation (Supplementary Figures 6–8C, G & K). Besides, RMSD plots of residues in the binding region were generated and the obtained results revealed that these residues maintained an overall stability in the studied complexes during 50 ns of MD simulation (Supplementary Figures 6–8D, H & L). Finally, deviations in measured RMSD values were lower than 2 Å, which indicated the overall stability of the studied complexes and that they undergo no significant conformational changes.

Moreover, to provide deeper stability analysis of the performed MD simulations, the number of hydrogen bond interactions in all systems was calculated [87]. Hydrogen bond (H-bond) was defined by the following criteria, representing the distance between donor and acceptor lower or equal to 3.5 Å and the angle lower or equal to 30°. As presented in Supplementary Figure 9, the observed H-bond interactions between the studied ligands and proteins were consistent throughout the 50 ns production run and were in agreement with those used for final analysis. Namely, clozapine was found to make only one H-bond interaction with all three studied targets through the whole run of 50 ns (Supplementary Figure 9A, D & G). This interaction was observed between clozapine and conserved amino acid Asp^{3×32} (Asp155 for 5-HT_{2A}-R, Asp114 for D₂-R and Asp107 for H₁-R). Moreover, from Supplementary Figure 9B, the authors conclude that the number of H-bonds between ziprasidone and 5-HT_{2A}-R remained stable after 25 ns until the end of the simulation, which is in concordance with the RMSD plots. On the other hand, D₂-R and H₁-R formed two interactions with ziprasidone that were stable from the beginning of the simulation (Supplementary Figure 9E & H). The number of H-bonds between lumateperone and 5-HT_{2A}-R fluctuated between two and three but remained at two for the last 20 ns (Supplementary Figure 9C). In accordance with the molecular docking study, lumateperone formed only one H-bond interaction with D₂-R and H₁-R, which was stable during all 50 ns of MD simulation (Supplementary Figure 9F & I). In summary, the high stability of H-bond interactions suggested good coupling between the studied complexes, without significant fluctuations during the simulated time.

To further examine the overall accuracy of the MD simulation results, the SASA of the binding sites was calculated. The SASA parameter could be used to describe the accessibility of the protein as well as to predict potential conformational changes [88]. The results, presented in Supplementary Figure 10, suggested that the SASA values were consistent in all studied complexes during the simulated time. For the last 25 ns, fluctuations were less

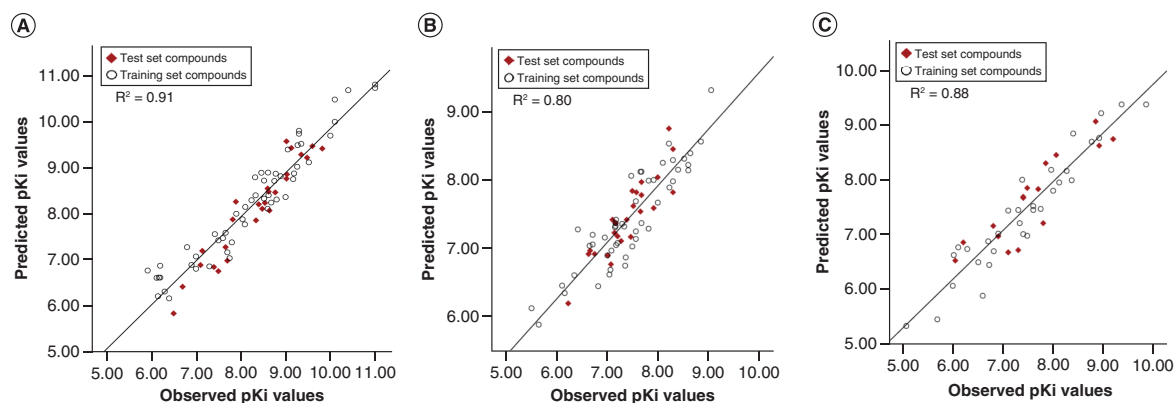


Figure 1. Plots of observed versus predicted negative logarithmic values of the inhibition constant for created 3D-quantitative structure–activity relationship models. (A) 5-HT_{2A} receptor. (B) D₂ receptor. (C) H₁ receptor. pKi: Negative logarithm of inhibition constant (-logKi).

than 4 nm² in all systems. Therefore, the obtained results additionally verified the stability of clozapine, ziprasidone and lumateperone in the binding sites of 5-HT_{2A}-R, D₂-R and H₁-R.

Overall, considering the results obtained from RMSD and SASA analysis, as well as H-bond measurements, the authors conclude that the performed MD simulations were long enough to reach equilibrium of the studied complexes during 50 ns of simulated time. Moreover, these findings indicated good stability of all trajectories, laying a good foundation for further molecular docking and 3D-QSAR studies.

After validation of the MD results, the last snapshot of each simulation was used to extract the antagonist-bound state of the receptor in complex with the reference ligand in its most probable bioactive conformation. The binding mode and molecular interactions of clozapine (Supplementary Figures 6–8A), ziprasidone (Supplementary Figures 6–8E) and lumateperone (Supplementary Figure 6–8I) within the active sites of 5-HT_{2A}-R, D₂-R and H₁-R were evaluated by the Discovery Studio Visualizer program. All essential interactions that play a significant role in 5-HT_{2A}-R, D₂-R and H₁-R binding were observed, including VdW interactions, H-bonding interactions and an electrostatic interaction with Asp^{3×32} (Asp155 for 5-HT_{2A}-R, Asp114 for D₂-R and Asp107 for H₁-R) [29–31].

Furthermore, all studied ligands were docked into the corresponding receptor conformation. The final ligand's pose was chosen based on the docking score and binding mode similar to the reference ligand. The results from the molecular docking studies are presented in Supplementary Tables 4–6.

With the aim to reproduce binding geometry of the co-crystallized ligands, the authors performed a redocking analysis. The obtained RMSD values were as follows: 0.764, 1.257 and 0.889 for 5-HT_{2A}-R–risperidone, D₂-R–risperidone and H₁-R–doxepin, respectively. Moreover, for further validation, the RMSD values of the heavy atoms between the docked and original conformations from MD simulations were calculated and the obtained values were 1.44, 0.64 and 1.54 for the 5-HT_{2A}-R–clozapine, 5-HT_{2A}-R–ziprasidone and 5-HT_{2A}-R–lumateperone complexes, respectively. Slightly better RMSD values were obtained for the D₂-R–clozapine, D₂-R–ziprasidone and D₂-R–lumateperone complexes: 0.20, 0.60 and 0.65, respectively. Additionally, RMSD values obtained for the H₁-R–clozapine, H₁-R–ziprasidone and H₁-R–lumateperone complexes were 1.18, 1.27 and 1.76, respectively. Since all values were below a widely accepted RMSD threshold value of 2.00 Å, the authors conclude that the results of the molecular docking analysis could be considered reliable [89].

3D-QSAR study

MD simulations followed by molecular docking studies were performed to more accurately predict the bioactive conformations of all studied ligands. The obtained conformers were used for calculation of the most important molecular descriptors that represent the structural features responsible for the relevant biological activity. In fact, three regression models were built, for 5-HT_{2A}-R, D₂-R and H₁-R, in order to describe the pharmacophore of dual 5-HT_{2A}/D₂-R antagonists with low affinity to H₁-R. The results are presented in Supplementary Tables 7–9, while the plots of observed versus predicted pKi values for the whole datasets are shown in Figure 1 (5-HT_{2A}-R [A], D₂-R model [B] and H₁-R [C] 3D-QSAR model).

Table 1. Results of internal and external validation of created 3D-quantitative structure–activity relationship models.

Model	Q ²	R ²	RMSEE	R ² _{pred}	RMSEP	r ² _m	r ² _m	r ² _m	Δr ² _m	(r ² –r ² ₀)/r ²	k'
5-HT _{2A} receptor	0.66	0.92	0.43	0.82	0.38	0.71	0.81	0.76	0.10	0.01	0.97
D ₂ receptor	0.61	0.81	0.36	0.77	0.25	0.69	0.76	0.72	0.08	0.00	1.01
H ₁ receptor	0.76	0.91	0.34	0.78	0.41	0.78	0.60	0.69	0.18	0.07	1.01
Criteria	>0.50	>0.70		>0.50	≤2 × RMSEE	>0.50	>0.50	>0.50	<0.20	<0.10	0.85 ≤ k' ≤ 1.15

K': (Σ Y_{obs} × Y_{pred})/Σ(Y_{obs})²; Q²: Cross-validated squared correlation coefficient; R²: Determination coefficient for training set; RMSEE: Root mean square error of estimation; R²_{pred}: Determination coefficient for test set; RMSEP: Root mean square error of prediction; r²_m: Coefficient of determination calculated according to equation 6; r²_m: Coefficient of determination calculated according to equation 7; r²_m: Average value of r²_m and r²_m; Δr²_m: Absolute difference between r²_m and r²_m; r²: r²_{metrics} determination coefficient (with intercept); r²₀: r²_{metrics} determination coefficient (without intercept); .

Table 2. Summary of the most important variables with positive and negative influence on 5-HT_{2A} receptor antagonistic activity.

Variable	Node pair	Distance (Å)	Comment
var176	N1-N1 (positive)	16.00–16.40	Two HBA groups at the optimal distance range, essential for more potent ligands from cluster 2
var257	TIP-TIP (positive)	21.20–21.60	Edge-to-edge distance in cluster 2 compounds that have significant enhancement potency toward 5-HT _{2A} receptor
var263	TIP-TIP (negative)	23.60–24.00	Unfavorable spatial distance between two steric regions in a few long-sized molecules
var288	DRY-O (positive)	6.40–6.80	Distance through molecule from hydrophobic region to protonated nitrogen as HBD in all studied compounds
var379	DRY-N1 (positive)	15.60–16.00	Most favorable distance between hydrophobic region and HBA, associated with the majority of compounds from clusters 2 and 3
var447	DRY-TIP (positive)	15.60–16.00	Similar to var257, representing a positive influence of optimal spatial distance between hydrophobic and steric regions in clusters 2 and 3
var460	DRY-TIP (negative)	20.80–21.20	Similar to var263, representing an unfavorable impact of hydrophobic and steric regions within longer spatial distance
var510	O-N1 (positive)	13.60–14.00	HBD and HBA groups positioned within the particular distance, in a majority of more potent compounds from cluster 2
var644	N1-TIP (negative)	12.80–13.20	Associated with less potent compounds from cluster 1 that have HBA and steric region at the lower distance range
var662	N1-TIP (positive)	20.00–20.40	Similar to var176 and var379, HBA group and steric region that are positioned at the defined distance; associated with cluster 2 compounds

DRY: Hydrophobic regions; HBA: Hydrogen bond acceptor; HBD: Hydrogen bond donor; N1: HBA regions; O: HBD regions; TIP: Steric hot spots.

In an effort to develop reliable and predictable 3D-QSAR models, an extensive statistical validation was performed (Table 1). High values of R² and Q² as well as low RMSEE values indicated good internal predictability for all created models. However, to demonstrate their real predictive capability, compounds from the test set were used for external model validation. The values of the following statistical parameters: R²_{pred}, r²_m, r²_m and r²_m greater than 0.50, Δr²_m value lower than 0.2 and low RMSEP values confirmed the predictive potential and stability of the created models, which could be employed for further quantitative activity prediction of the new analogues.

The PLS coefficient plots describing the contribution of each variable in the model are shown in Supplementary Figures 11–13. The most important variables for the model interpretation are marked with numbers and described in Tables 2–4. Variables with the positive coefficients are in direct correlation to biological activity, while those with negative coefficients possess an opposite correlation.

Pharmacophore analysis of 5-HT_{2A}-R ligands

A 3D-QSAR model for 5-HT_{2A}-R enabled the authors to deeply analyze the crucial structural features required for the high binding affinity of the studied antagonists. Compared with others, the lower potency of the compounds from cluster 1 on this receptor (pK_{i5-HT_{2A}-R}: 5.92–8.80) can be described with the presence of the only positive variable, DRY-O (var288) (Figure 2A). This variable emphasizes the distance through molecule from the hydrophobic region to protonated nitrogen as HBD. A less potent compound from this group, ChEMBL1277585, possesses a high value of the negative N1-TIP (var644) variable (Figure 2B), indicating an unfavorable impact of HBA and

Table 3. Summary of the most important variables with positive and negative influence on D₂ receptor antagonistic activity.

Variable	Node pair	Distance (Å)	Comment
var43	DRY-DRY (negative)	17.20–17.60	Unfavorable interaction between two hydrophobic regions at a longer distance
var149	N1-N1 (positive)	7.60–8.00	Optimal distance between two HBA groups, essential for more potent ligands
var296	DRY-O (positive)	14.40–14.80	Hydrophobic region and HBD group within the particular distance, characteristic for cluster 2 compounds
var422	DRY-TIP (positive)	12.80–13.20	Most favorable distance between hydrophobic and steric regions, inherent in more potent compounds from clusters 2 and 3
var440	DRY-TIP (negative)	20.00–20.40	Similar to var43, representing a negative influence of longer spatial distance between hydrophobic and steric regions
var470	O-N1 (positive)	6.00–6.40	HBD and HBA groups positioned within the particular distance, presented in all three clusters
var534	O-TIP (negative)	5.60–6.00	Present for the majority of less potent compounds from cluster 1 that have HBD and steric region at lower distance range
var551	O-TIP (positive)	12.40–12.80	Distance through molecule between protonated nitrogen as HBD and steric region for all three clusters
var563	O-TIP (positive)	17.20–17.60	Similar to var296, HBD group and steric region that are positioned at the defined distance; associated with cluster 2 compounds
var635	N1-TIP (positive)	20.00–20.40	Present for the majority of cluster 2 and 3 compounds, describing HBA and steric regions within defined spatial distance.

DRY: Hydrophobic regions; HBA: Hydrogen bond acceptor; HBD: Hydrogen bond donor; N1: HBA regions; O: HBD regions; TIP: Steric hot spots.

Table 4. Summary of the most important variables with positive and negative influence on H₁ receptor antagonistic activity.

Variable	Node pair	Distance (Å)	Comment
var149	N1-N1 (negative)	10.00–10.40	Negative influence of two HBA groups within defined distance range, related to cluster 2 compounds
var217	TIP-TIP (positive)	12.40–12.80	Edge-to-edge distance of cluster 1 compounds that have positive influence on H ₁ receptor binding activity
var237	TIP-TIP (negative)	20.40–20.80	Edge-to-edge distance of cluster 2 compounds that negatively correlates with H ₁ receptor binding activity
var275	DRY-O (positive)	10.80–11.20	Distance through molecule between protonated nitrogen as HBD and steric region, essential for all compounds
var343	DRY-N1 (negative)	13.20–13.60	Unfavorable distance between hydrophobic region and HBA group, mostly characteristic for cluster 2 compounds
var398	DRY-TIP (positive)	10.40–10.80	Similar to var217; defines optimal spatial distance between hydrophobic and steric region in molecule
var408	DRY-TIP (negative)	14.40–14.80	Represents longer distance range between hydrophobic and steric region, inherent in cluster 2 compounds
var458	O-N1 (negative)	9.60–10.00	Similar to var149, unfavorable distance between HBD and HBA groups presented in cluster 2 compounds
var534	O-TIP (negative)	15.20–15.6	Negative impact of shorter distance between HBD (carboxyl) group and steric region presented in cluster 1 compounds
var599	N1-TIP (negative)	16.40–16.80	Similar to var149 and var458, associated with cluster 2 compounds that have HBA and steric region at the defined distance range

DRY: Hydrophobic regions; HBA: Hydrogen bond acceptor; HBD: Hydrogen bond donor; N1: HBA regions; O: HBD regions; TIP: Steric hot spots.

steric region at the lower distance range. Moreover, these compounds lack important positive variables, such as N1-N1 (var176), TIP-TIP (var257), DRY-N1 (var379), DRY-TIP (var447), O-N1 (var510) and N1-TIP (var662), which are expressed for the majority of the more potent ligands as in cluster 2 (pKi: 7.00–11.00) and cluster 3 (pKi: 6.15–9.27). Briefly, these variables define optimal distance through molecule between hydrophobic, steric and H-bond donating regions in medium-sized molecules, such as ziprasidone and lumateperone (Figure 2C & E). The variables TIP-TIP (var257: 21.20–21.60 Å) and DRY-TIP (var447: 15.60–16.00 Å) define optimal edge-to-edge distance of more potent molecules (Figure 2C & E). They indicate that the presence of two heterocyclic rings

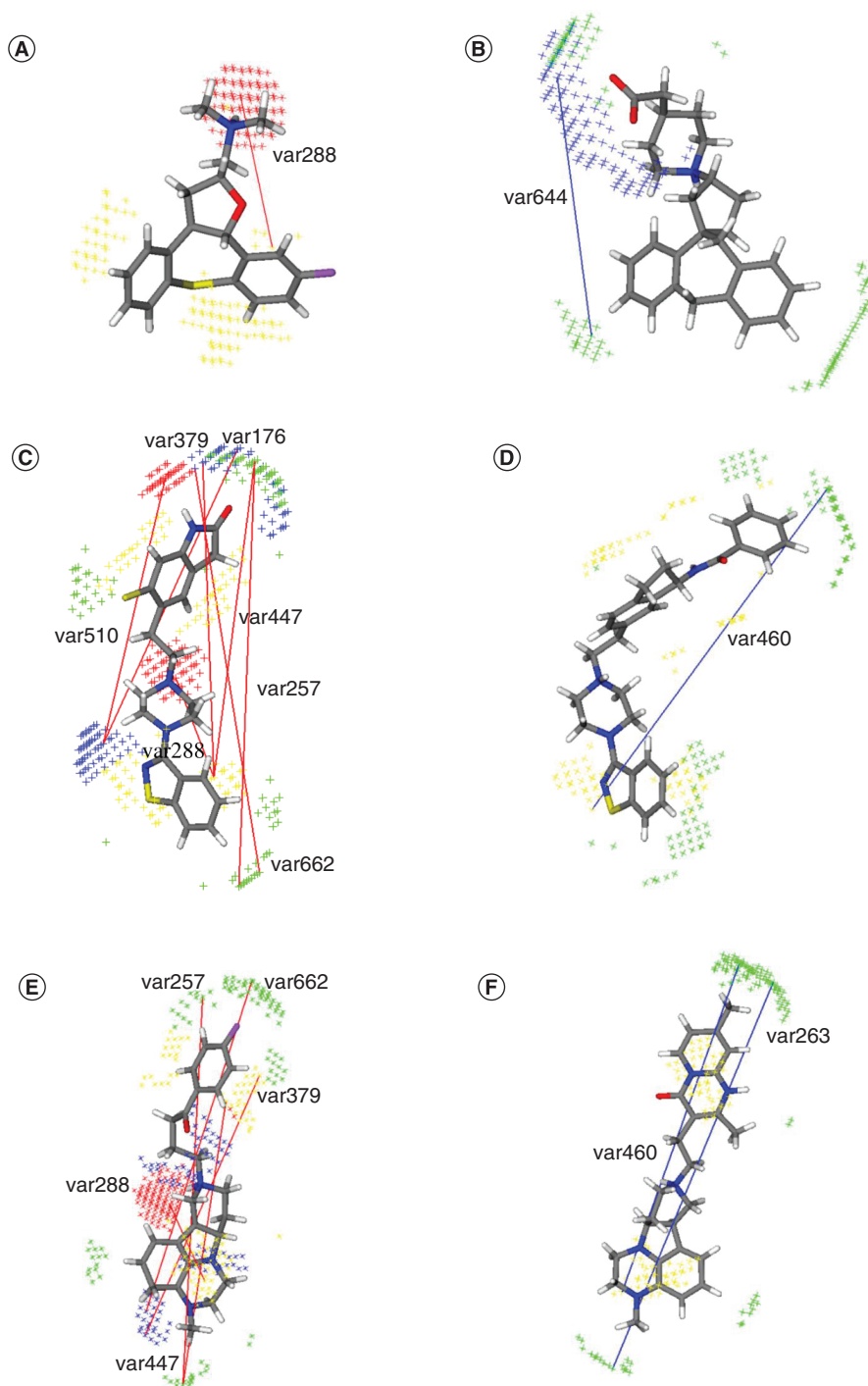


Figure 2. The most important positive (red) and negative (blue) variables from created 3D-quantitative structure–activity relationship model for 5-HT_{2A} receptor. (A) ChEMBL366164 and (B) ChEMBL1277585 from cluster 1. (C) ChEMBL708-ziprasidone and (D) ChEMBL253233 from cluster 2. (E) ChEMBL3233142-lumateperone and (F) ChEMBL3233416 from cluster 3. The steric hot spots (TIP) are presented in green, hydrophobic regions (DRY) in yellow, hydrogen bond acceptor regions (N1) in blue and hydrogen bond donor regions (O) in red.

at a particular distance possesses significant enhancement potency toward this receptor. In contrast, the negative variables TIP-TIP (var263: 23.60–24.00 Å) and DRY-TIP (var460: 20.80–21.20 Å) imply that any increase in the distance between these regions might lead to a decrease in the biological activity of 5-HT_{2A}-R antagonists (Figure 2D & F). Furthermore, the majority of more potent molecules have an HBA group, mainly carboxyl, at

the optimal spatial distance from one of the molecular termini, as described by variables DRY-N1 (var379: 15.60–16.00 Å) and N1-TIP (var662: 20.00–20.40 Å) (Figure 2C & E). Additionally, the importance of H-bonding interactions in the binding site of 5-HT_{2A}-R was confirmed with variables N1-N1 (var176: 16.00–16.40 Å) and O-N1 (var510: 13.60–14.00 Å) (Figure 2C). They represent HBA and HBD groups of both heterocyclic rings positioned within a particular distance, associated with more potent compounds. Confirming the reliability of the created 3D-QSAR model, variable DRY-O (var288: 6.40–6.80 Å) was pronounced in all studied compounds describing the importance of protonated nitrogen atom which form an essential interaction with highly conserved aspartic acid (Asp^{3×32}) [90]. Detailed interpretation of each variable is provided in the supporting material.

Interactions in the binding site of 5-HT_{2A}-R

A further molecular docking study was performed with the aim to support the conclusions from 3D-QSAR analysis. 5-HT_{2A}-R–clozapine complex conformation was used to dock ligands from cluster 1 (Figure 3A & B), while ligands from cluster 2 (Figure 3C & D) and cluster 3 (Figure 3E & F) were docked into 5-HT_{2A}-R–ziprasidone and 5-HT_{2A}-R–lumateperone conformations, respectively. Detailed binding mode interaction of the studied antagonists is provided in the supporting material. In summary, the tricyclic ring of compounds from cluster one occupies only the bottom hydrophobic cleft of 5-HT_{2A}-R defined with the key residues on TM3, TM5 and TM6: Val156^{3×33}, Ser159^{3×36}, Thr160^{3×37}, Ile163^{3×40}, Ile210^{4×61}, Phe234^{5×39}, Ile237^{5×42}, Gly238^{5×43}, Ser242^{5×461}, Phe243^{5×47}, Trp336^{6×48} and Phe340^{6×52} (Figure 3A & B). However, the introduction of another hydrophobic moiety above the salt bridge involves an extended conformation in the binding site of 5-HT_{2A}-R (Figures 3C–F). Amino acids such as Ser131^{2×60}, Ile135^{2×64}, Tyr139, Trp151^{3×28}, Ile152^{3×29}, Leu228^{45×51}, Leu229^{45×52}, Asn363^{7×35}, Val366^{7×38} and Tyr370^{7×42} on TM2, TM3, ECL2 and TM7 enclose the oxindole ring and benzene ring of ziprasidone and lumateperone, respectively (Figure 3C & E). The created 3D-QSAR model extracted TIP-TIP (var263) and DRY-TIP (var460) variables, which imply that the presence of these heterocyclic rings positively correlates with 5-HT_{2A}-R binding affinity. All compounds exhibited strictly conserved electrostatic interaction between Asp155^{3×32} and the protonated nitrogen of the piperazine ring (Figure 3), previously confirmed with a 3D-QSAR study (DRY-O, var288). Furthermore, the majority of the more potent compounds from cluster 2, which possess a carboxyl group, such as ziprasidone, were found to make H-bond interactions with Asn363^{7×35} (Figure 3C). The importance of this polar interaction was also confirmed with extracted variables from the 3D-QSAR model (N1-N1, var176; DRY-N1, var379; and N1-TIP, var662) as well as with the authors' previous study [35].

Pharmacophore analysis of D₂-R ligands

Analysis of the most important GRIND variables with positive and negative influence on biological activity provided insight into the basic ligand structural requirements for high binding affinity to D₂-R. Generally, compounds from cluster 1 (pKi: 5.66–8.64) are less potent compared with compounds from cluster 2 (pKi: 7.17–9.05). 3D-QSAR model analysis showed that N1:N1 (var149), O-N1 (var470) and O-TIP (var551) variables possess a strong positive influence on the potency of molecules from cluster 1 (Figure 4A). GRIND variable N1-N1 (var149: 7.60–8.00 Å) describes the proximity between two HBA groups, the oxygen atom of the dibenzoxepin ring and the nitrogen atom of the piperazine ring (Figure 4A). The significance of the protonated nitrogen atom of the piperazine ring in the binding affinity was confirmed with variables O-N1 (var470: 6.00–6.40 Å) and O-TIP (var551: 12.40–12.80 Å) (Figure 4A). However, their lower activity can be described with the absence of the important positive variables such as DRY-O (var296), O-TIP (var563) and N1-TIP (var635), as well as high values of negative variable O-TIP (var534) (Figure 4B), calculated for compounds bearing a shorter distance between protonated nitrogen as HBD and terminal methyl group as a steric hot spot (Figure 4B). Through analysis of the most active compounds from cluster two, ziprasidone and cluster three, ChEMBL3233413, the authors concluded that the introduction of two heterocyclic rings, at the optimal distance range of 12.80–13.20 Å defined with var422 (DRY-TIP), increases the potency of compounds toward D₂-Rs (Figure 4C & E). This may contribute to better ligand fitting into the receptor binding site. Further increase in spatial distance between hydrophobic and steric regions or two hydrophobic regions shows diminutive effect on the biological activity (var440, DRY-TIP: 20.00–20.40 Å; var43, DRY-DRY: 17.20–17.60 Å) (Figure 4D & F). Moreover, variables such as var149 (N1-N1: 7.60–8.00 Å), var296 (DRY-O: 14.40–14.80 Å), var470 (O-N1: 6.00–6.40 Å), var563 (O-TIP: 17.20–17.60 Å) and var635 (N1-TIP: 20.00–20.40 Å) imply that the presence of HBA and HBD groups in both heterocyclic rings may be important for establishing favorable H-bonding interactions with the polar amino acids in the active pocket (Figure 4C). Nevertheless, the absence of HBD and HBA groups at the optimal spatial distance from the tetracyclic

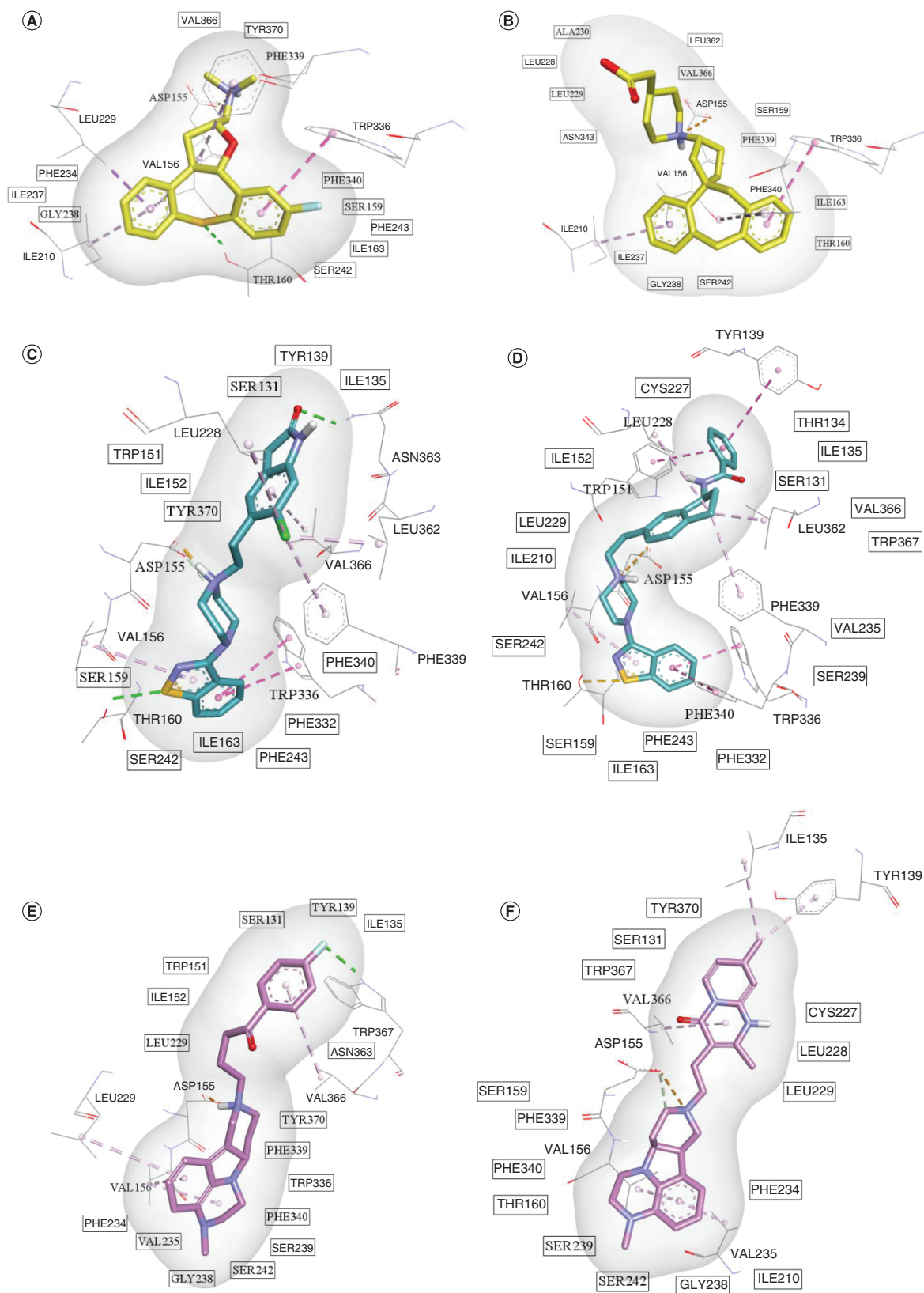


Figure 3. Representation of binding modes in the active site of 5-HT_{2A} receptor. (A) ChEMBL366164. (B) ChEMBL1277585. (C) ChEMBL708–ziprasidone. (D) ChEMBL253233. (E) ChEMBL3233142–lumateperone. (F) ChEMBL3233416. The π - π and alkyl- π interactions are depicted in purple, hydrogen bond interactions in green and salt bridge in orange. Outlined amino acids form Van der Waals interactions.

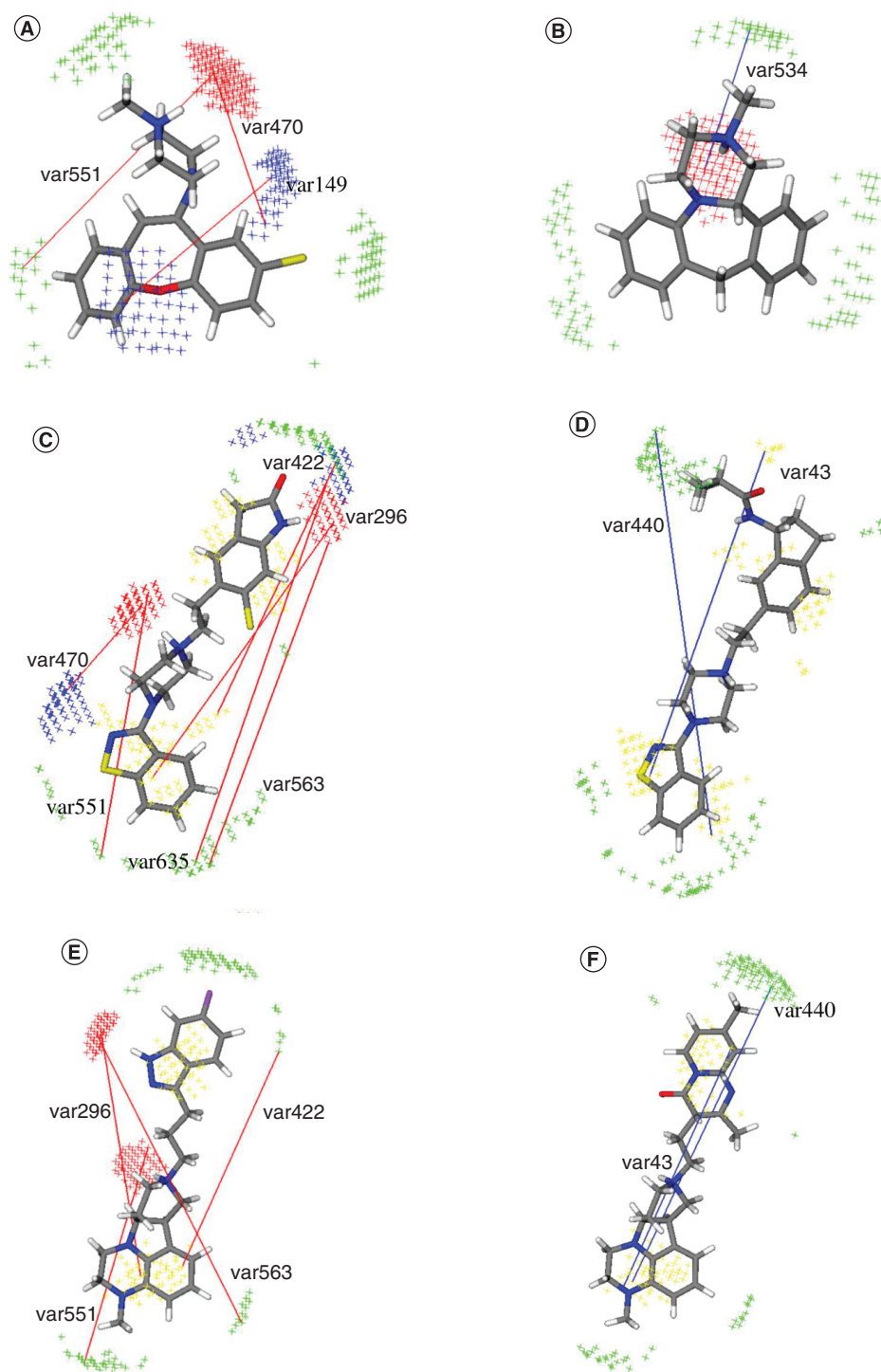


Figure 4. The most important positive (red) and negative (blue) variables from created 3D-quantitative structure–activity relationship model for D₂ receptor. (A) ChEMBL90882 and (B) ChEMBL6437 from cluster 1. (C) ChEMBL708-ziprasidone and (D) ChEMBL400236 from cluster 2. (E) ChEMBL3233413 and (F) ChEMBL3233416 from cluster 3. The steric hot spots (TIP) are presented in green, hydrophobic regions (DRY) in yellow, hydrogen bond acceptor regions (N1) in blue and hydrogen bond donor regions (O) in red.

ring potentially affected the potency of compounds from cluster 3. Notably, var551 (O-TIP: 12.40–12.80 Å) was expressed in all ligands describing distance through molecule from the protonated nitrogen atom as HBD to the steric region around the heterocyclic ring. A detailed description of each variable is presented in the supporting material.

Interactions in the binding site of D₂-R

Furthermore, the molecular docking method was used to reveal interactions in the binding site between the studied ligands and D₂-R, as well as to compare the obtained findings with 3D-QSAR pharmacophore analysis. Cluster 1 compounds were docked into D₂-R–clozapine complex conformation, and the binding modes of ChEMBL90882 and ChEMBL6437 are presented in Figure 5A & B. Conformation of D₂-R in complex with ziprasidone was used to dock ligands from cluster 2 (Figure 5C & D), while tetracyclic quinoxaline derivatives from cluster 3 were docked into D₂-R conformation after MD simulation with lumateperone (Figure 5E & F). Integrating the binding mode analyses of structurally diverse antagonists, presented in the supporting material, the authors summarized that compounds with two heterocyclic rings at the optimal distance perfectly fit into the active pocket of D₂-R defined with residues from TM2, 3, 5, 6 and 7 and ECL1 [30,32,91]. Unlike cluster 2 and 3 compounds, polycyclic aromatic derivatives from cluster 1 show weaker affinity for D₂-R, which may be confirmed with lower values of AD Vina docking scores (Supplementary Table 5). All compounds form a salt bridge interaction with Asp114^{3×32}, while only those that possess an HBD group, at a certain distance from the hydrophobic region, were found to make an H-bond interaction with Ser409^{7×35}. This interaction is inherent in more potent compounds, as demonstrated with several variables in the 3D-QSAR study (DRY-O, var296; O-TIP, var563). Moreover, it may be important for maintaining the stability of a ligand in complex with D₂-R, as well as binding selectivity.

Comparative analysis of 3D-QSAR & molecular docking results for 5-HT_{2A}-Rs, D₂-Rs & H₁-Rs

Additionally, to fulfill the criteria of multi-target ligands with a desired selectivity profile, the authors performed 3D-QSAR and molecular docking studies on known H₁-R antagonists (Figure 6). A further focus of the study was to compare the obtained results with findings from 5-HT_{2A}-R and D₂-R analyses.

Both, 5-HT_{2A}-R and D₂-R 3D-QSAR models revealed a favorable distance range between two heterocyclic rings, beneficial for high binding affinity, through variables TIP-TIP (var257) and DRY-TIP (var447) from the 5-HT_{2A}-R study and DRY-TIP (var422) from the D₂-R study. On the other hand, the 3D-QSAR model for H₁-R revealed that the presence of two hydrophobic regions at a longer spatial distance leads to a decrease in biological activity (TIP-TIP, var237; DRY-TIP, var408) (Figure 6B). Moreover, GRIND variables TIP-TIP (var217) and DRY-TIP (var398) describing the molecular shape of small-sized molecules of cluster 1 positively correlate with H₁-R antagonistic activity (Figure 6A). These findings agree well with experimentally obtained results showing that clozapine-like compounds (cluster 1) are more potent on H₁-Rs compared with 5-HT_{2A}-Rs and D₂-Rs, whereas it is the opposite for ziprasidone-like compounds (cluster 2). Furthermore, the docking scores of cluster 1 compounds in complex with H₁-R (Supplementary Table 6) were significantly higher than those obtained with docking into 5-HT_{2A}-R (Supplementary Table 4) and D₂-R (Supplementary Table 5).

Based on insights gained from the created 3D-QSAR models for 5-HT_{2A}-R and D₂-R, the authors concluded that the presence of HBD and HBA groups at the optimal distance from the heterocyclic ring, which also possesses HBA properties, may significantly increase the bioactivity of dual antagonists. GRIND variables DRY-N1 (var379) and N1-TIP (var662) from the 5-HT_{2A}-R 3D-QSAR model as well as N1-TIP (var635) from the D₂-R 3D-QSAR model precisely describe distance through molecule between HBA group and heterocyclic ring, which perfectly fits into the bottom hydrophobic cleft. In addition, O-N1 (var510, 5-HT_{2A}-R), DRY-O (var296, D₂-R) and O-TIP (var563, D₂-R) variables highlight the importance of the HBD group at a similar distance range. In contrast, the H₁-R model revealed that variables N1-N1 (var149), DRY-N1 (var343), O-N1 (var458), O-TIP (var534) and N1-TIP (var599) have a negative impact on bioactivity, suggesting that the presence of these groups may contribute to better selectivity of dual antagonists.

To facilitate a comparison between the studied receptors, the GPCR database was used to align residues in the binding site by their position (Supplementary Figure 14) [92]. As demonstrated in Supplementary Figure 14, highly conserved residues among the studied aminergic receptors are at positions 3×32, 3×40, 6×44, 6×48 and 6×52. However, certain differences were observed at positions 3×33 and 5×40 of H₁-R, where residues Tyr108 and Lys191, respectively, may form H-bond interactions and contribute to high affinity binding to H₁-R [31]. Besides, at position 7×35, both 5-HT_{2A}-Rs and D₂-Rs possess polar amino acids, Asn363 and Ser409, respectively, whereas

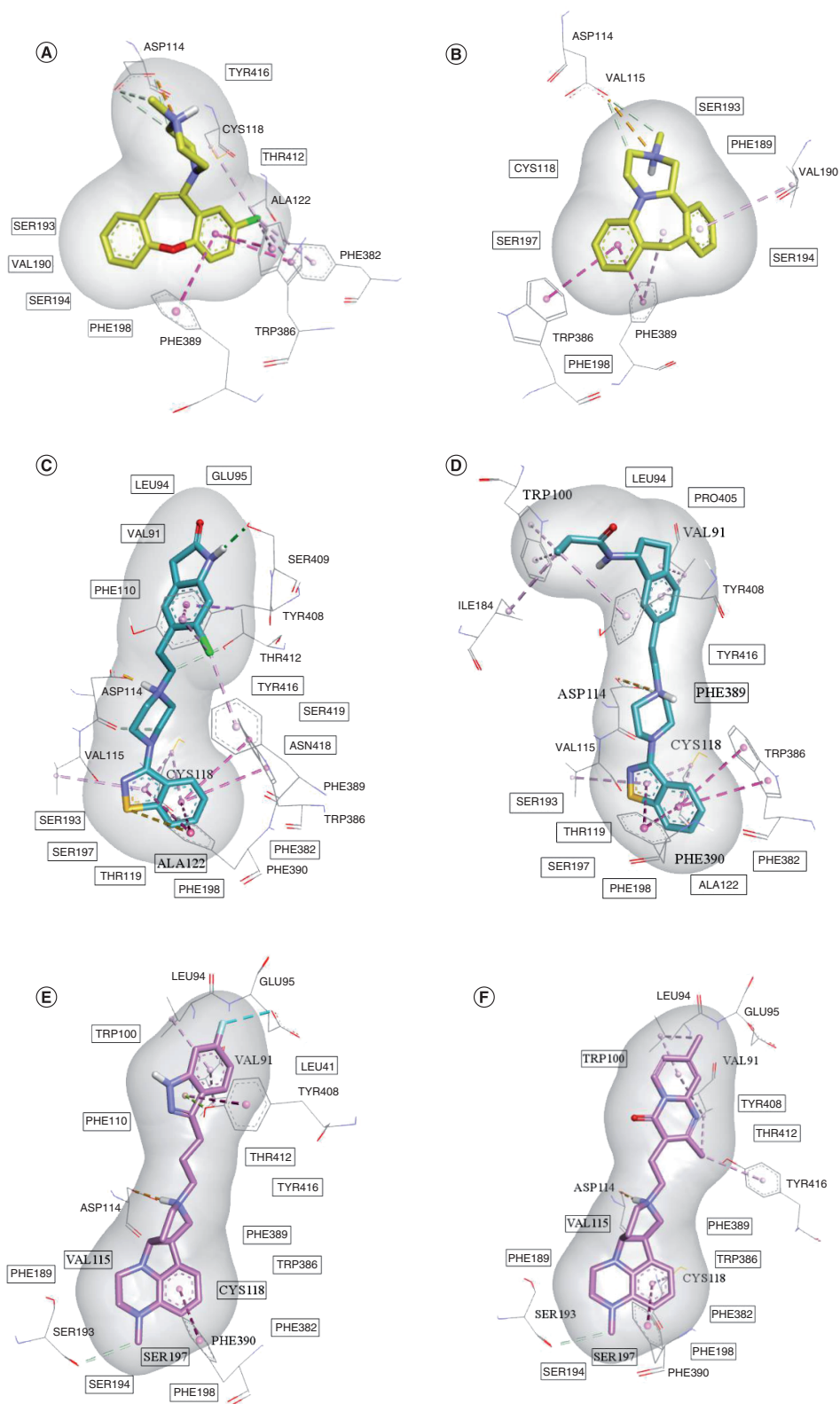


Figure 5. Representation of binding modes in the active site of D₂ receptor. (A) ChEMBL90882. (B) ChEMBL6437. (C) ChEMBL708-ziprasidone. (D) ChEMBL400236. (E) ChEMBL3233413. (F) ChEMBL3233416 in the active site of D₂ receptor. The π - π and alkyl- π interactions are depicted in purple, hydrogen bond interactions in green and salt bridge in orange. Outlined amino acids form Van der Waals interactions.

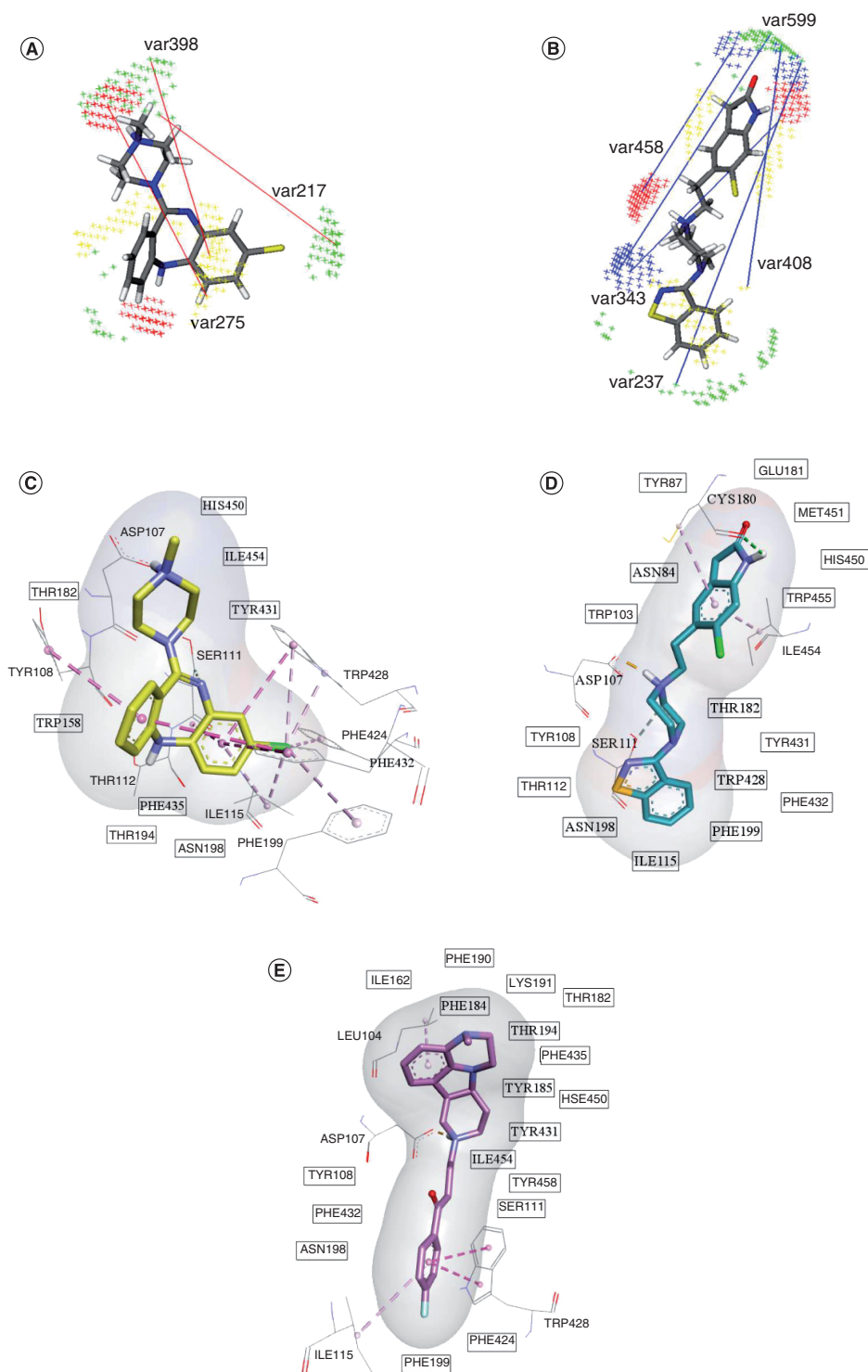


Figure 6. 3D-quantitative structure-activity relationship analysis and molecular docking study for H₁ receptor. The most important positive (red) and negative (blue) variables for ChEMBL42-clozapine (A) and ChEMBL708-ziprasidone (B), obtained from the created 3D-quantitative structure-activity relationship model. The steric hot spots (TIP) are presented in green, hydrophobic regions (DRY) in yellow, hydrogen bond (H-bond) acceptor regions (N1) in blue and H-bond donor regions (O) in red. Representation of binding modes of ChEMBL42-clozapine (C), ChEMBL708-ziprasidone (D) and ChEMBL3233142-lumateperone (E) within H₁ receptor. The π - π and alkyl- π interactions are depicted in purple, H-bond interactions in green and salt bridge in orange. Outlined amino acids form Van der Waals interactions.

H₁-Rs have Met451. Unlike methionine, which forms only hydrophobic interactions, asparagine and serine can make H-bond interactions with ligands in the binding site. This finding is in concordance with previously described 3D-QSAR variables as well as molecular docking results that revealed interaction with these residues. Moreover, all created 3D-QSAR models underline the importance of tertiary amine as HBD, which interacts with Asp155 for 5-HT_{2A}-R, Asp114 for D₂-R and Asp107 for H₁-R at position 3×32 (var288, 5-HT_{2A}-R; var551, D₂-R; and var275, H₁-R).

In addition, to inspect the binding interactions of lumateperone in the active site of H₁-R, the authors performed MD and molecular docking studies (Figure 6E). They demonstrated that it occupies the binding site of H₁-R in the opposite conformation from binding to D₂-R and 5-HT_{2A}-R, therefore involving more hydrophobic interactions in the upper hydrophobic cleft (Figure 6E). Unlike clozapine, which is a tricyclic derivate and fits much deeper in the lower aromatic region of the H₁-R, lumateperone forms fewer hydrophobic contacts with residues in this binding site (Figure 6C & E). In particular, non-conserved residue Trp158^{4×57} as well as Thr112^{3×37} were not found to interact with lumateperone. Furthermore, compared with ziprasidone, which exhibits H-bond interaction with Cys180 in ECL2, lumateperone was not observed to form any electrostatic interaction within the H₁-R active pocket (Figure 6D & E). All these factors contribute to the fact that lumateperone possesses a higher selectivity profile for off-target histaminergic receptors compared with other antipsychotic medications [93].

Finally, the results obtained from the molecular docking and 3D-QSAR studies are complementary and validated each other, revealing that the developed structure–activity relationship models for 5-HT_{2A}-R, D₂-R and H₁-R are reliable and may be further used to accelerate the design and identification of novel, potent dual antagonists of 5-HT_{2A}/D₂-Rs, with minimized activity on the histamine H₁-R.

Applicability domain

As described in the ‘Materials & methods’ section, the leverage approach was performed to examine and visualize the applicability domain of all the created 3D-QSAR models. The ten most important variables of each model were extracted and the warning leverage values were calculated (0.61 for the 5-HT_{2A}-R model, 0.63 for the D₂-R model and 0.97 for the H₁-R model). The Williams plots in Supplementary Figures 15–17 suggest that neither training nor test set compounds deviated from the determined domain of applicability. In conclusion, all developed 3D-QSAR models could be further used for reliable activity prediction of new, structurally similar compounds.

Rational drug design of new dual antagonists

The integrated use of MD, molecular docking and 3D-QSAR methods enabled the authors to compressively investigate the pharmacophore of dual 5-HT_{2A}/D₂-R antagonists with low H₁-R activity. The obtained findings suggest that longer edge-to-edge distance of molecules showed a positive correlation with 5-HT_{2A}/D₂-R binding activity, whereas it negatively correlated with H₁-R activity. Furthermore, the presence of a heterocyclic ring (A) with the HBA sites (such as heterocyclic nitrogen or oxygen atoms) at the optimal distance range from another ring (B), which contains HBA but also HBD groups, could enhance ligand binding activity toward 5-HT_{2A}-Rs and D₂-Rs (Figure 7). Molecular docking studies showed that these groups form important H-bonding interactions with residues at positions 3×37 (Thr160 for 5-HT_{2A}-R and Thr119 for D₂-R) and 7×35 (Asn363 for 5-HT_{2A}-R and Ser409 for D₂-R) in the bottom and upper hydrophobic cleft, respectively. In contrast, 3D-QSAR study analysis revealed that the introduction of such substituents at longer distances decreases H₁-R activity. Binding site analysis of the studied targets also showed that differences in amino acid composition, especially at position 7×35 (Met451 for H₁-R), have an important impact on achieving selectivity of dual antagonists against H₁-R.

Following the determination of the crucial structural features for dual antagonists, design strategies were based on modifications of two hydrophobic regions, A and B, separated with a well-established piperazine linker with a positively charged nitrogen atom, important to retain an optimal aminergic receptor activity profile (Figure 7). ChEMBL90882, ziprasidone and lumateperone were selected as lead compounds. Additionally, the authors employed the FBDD method to design novel potent compounds with good drug-like properties. Templates, 1,2-benzothiazol and dibenzoxepin for hydrophobic region A, as well as 1,3-dihydro-2-oxindol for hydrophobic region B, were chosen as attractive starting points, which possess a characteristic interaction profile with the studied targets (Supplementary Table 10). They represent fragments of lead molecules, ChEMBL90882 and ziprasidone, which perfectly fit into the hydrophobic binding pocket of the studied 5-HT_{2A}-Rs and D₂-Rs and form important H-bond interactions in the active sites. With this in mind, the authors’ aim was to explore different fragments from available databases (General Fragment Library and Enamine Essential Fragment Library) by their similarity

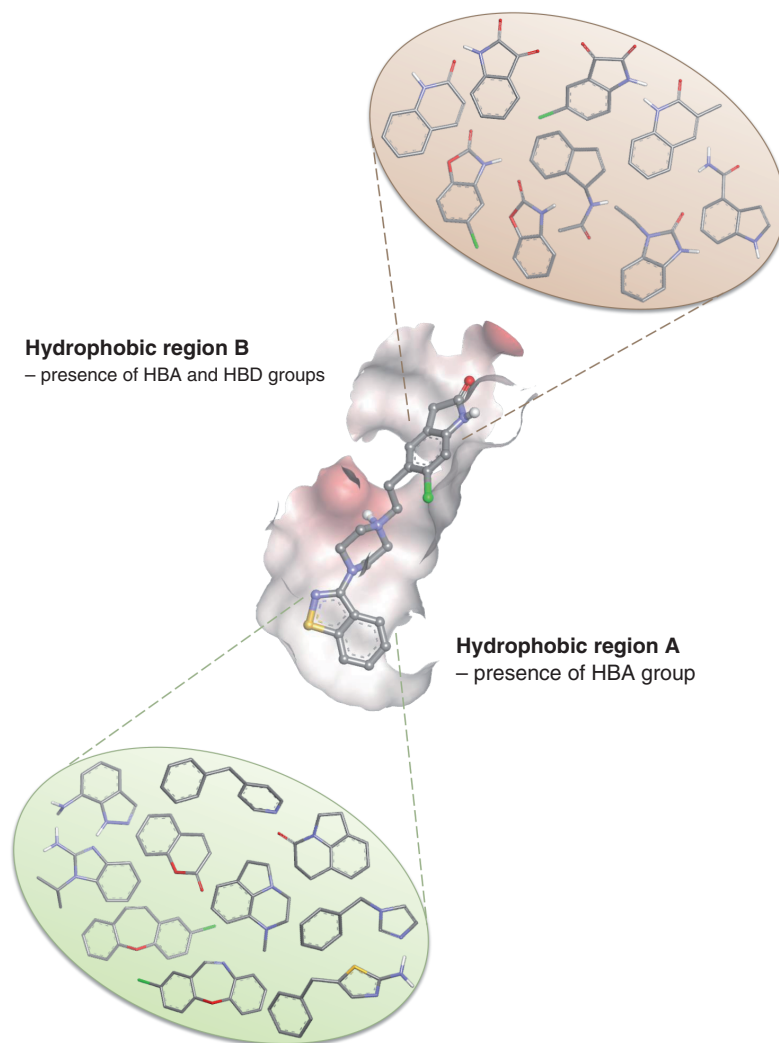


Figure 7. The general strategies employed for rational design of novel dual 5-HT_{2A}/D₂ receptor antagonists with low affinity toward the H₁ receptor, obtained after overall *in silico* analysis.

HBA: Hydrogen bond acceptor; HBD: Hydrogen bond donor.

to the selected templates. The 14 fragment hits with the highest similarity score (Glob-Sum) values were chosen for replacement of hydrophobic regions A and B. The selected fragments along with the Glob-Sum values are presented in Supplementary Table 10.

30 new molecules were designed by modification of lead compounds or by linking two fragments with ethyl piperazine in order to retain optimal distance between them but also to establish stronger H-bond interactions with targets of interest (Supplementary Figure 18). Furthermore, they were optimized and docked in the same manner as the dataset molecules. Depending on similarity to the reference ligand from the MD simulation, designed compounds were docked into each receptor (5-HT_{2A}, D₂ and H₁) using the AD Vina program, and the obtained docking scores are presented in Supplementary Table 11. Afterward, the created 3D-QSAR models of all three receptors were used to predict their pK_i values (Supplementary Table 11).

Based on the activity predictions, three structurally different compounds, A2, B3 and C3, were selected for further molecular docking analysis. Not only were these compounds predicted to have a similar or higher affinity for 5-HT_{2A}-Rs and D₂-Rs as lead molecules, but also they were found to exhibit significantly higher differences between predicted pK_i values for 5-HT_{2A}/D₂-Rs and off-target H₁-R compared with others (Supplementary Table 11). With this in mind, the molecular docking approach was further used to analyze the key interactions of A2, B3 and C3 molecules in the active sites of 5-HT_{2A}-Rs, D₂-Rs and H₁-Rs (Figure 8). All three ligands

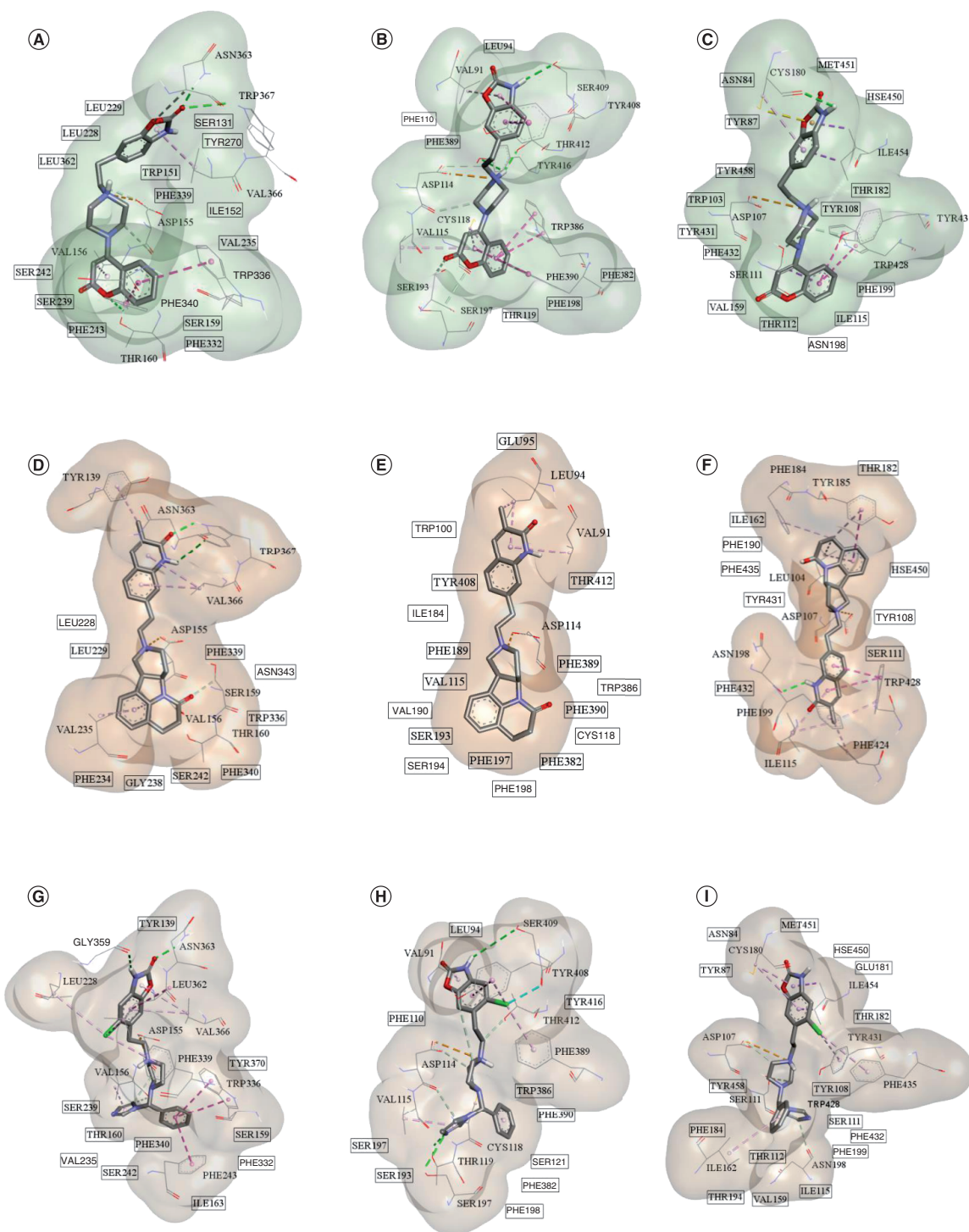


Figure 8. Representation of molecular docking results for designed compounds. A2 in complex with 5-HT_{2A}-R (A), D₂ receptor (D₂-R) (B) and H₁ receptor (H₁-R) (C); B3 in complex with 5-HT_{2A}-R (D), D₂-R (E) and H₁-R (F); and C3 in complex with 5-HT_{2A}-R (G), D₂-R (H) and H₁-R (I). The hydrogen bond interactions are depicted in green, salt bridge in orange, and π - π and alkyl- π interactions in purple. Outlined amino acids form Van der Waals interactions.

possess aromatic heterocyclic rings in the bottom hydrophobic cleft, which form CH- π , π - π or hydrophobic interactions with all essential residues. Additional H-bond interactions with residues at positions 3 \times 37 (Thr160 for 5-HT_{2A}-R and Thr119 for D₂-R), 5 \times 43 (Ser193 for D₂-R) and 5 \times 461 (Ser197 for D₂-R) were observed for all three compounds, due to the presence of the HBA group (Figures 8A, B, D & H). However, in the active site of H₁-R, only compound B3 formed an interaction with Asn198^{5 \times 461} (Figure 8F). Moreover, it was observed that the charged tertiary nitrogen atom of the piperazine ring of the designed compounds formed the crucial interaction with Asp^{3 \times 32} (Asp155, Asp114 and Asp107 for 5-HT_{2A}-Rs, D₂-Rs and H₁-Rs, respectively) (Figure 8). Since the 3D-QSAR studies showed that the introduction of hydrophobic region B leads to an increase in 5-HT_{2A}-R and D₂-R activity and a decrease in H₁-R activity, different fragments were investigated in this position. All of them were perfectly embedded within the hydrophobic pocket comprised of TM2, TM3, TM7 and ECL2 for 5-HT_{2A}-R or ECL1 for D₂-R (Figure 8). Moreover, the aforementioned analysis emphasized that the introduction of HBD and HBA groups positively correlates with 5-HT_{2A}-R and D₂-R activity, compared with H₁-R. As shown in Figure 8A, D & G, all three selected compounds form H-bond interactions with Asn363^{7 \times 35} of 5-HT_{2A}-R. Additionally, carbonyl oxygen of the 2-benzoxazolinone moiety of A2 and 2-oxoquinoline of B3 molecules interact with Trp367^{7 \times 39}, while -NH of the C3 molecule forms an H-bond with Gly359^{7 \times 31}. Furthermore, docking into D₂-R shows that A2 and C3 ligands make contact with polar residue Ser409^{7 \times 35}, which is at the same position as Asn363 of 5-HT_{2A}-R (Figure 8B & H). In contrast, the 3D-QSAR study suggested that the presence of these groups has a negative impact on H₁-R activity. A docking study revealed that only the A2 compound forms an H-bond interaction with Cys180^{45 \times 50} from ECL2 of H₁-R. Generally, all designed compounds possess higher 5-HT_{2A}-R than D₂-R activity, which may be beneficial for optimal efficacy and lower propensity to cause side effects such as EPSs. It is worthy to note that these ligands were also predicted to have significantly lower H₁-R activity compared with ziprasidone and clozapine (Supplementary Table 11).

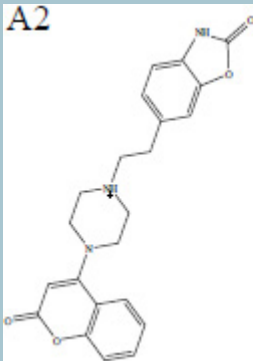
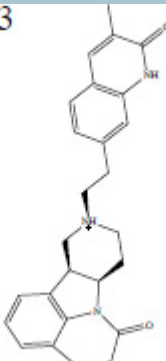
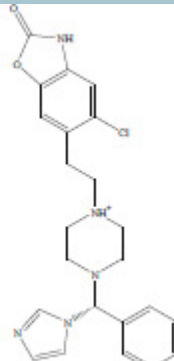
The leverage approach was employed to examine if the designed compounds fall within the defined applicability domain for each receptor. As presented in Supplementary Figures 19–21, the authors conclude that there are no outliers and predicted pKi values may be considered reliable.

In silico prediction of ADMET properties for designed compounds

After activity predictions, different physico-chemical parameters, synthetic difficulty scores (Supplementary Table 12) and pharmacokinetic properties (Supplementary Table 13) were calculated for *in silico* evaluation of novel designed antagonists by using ADMET Predictor software. The lipophilicity features were assessed by MlogP and LogP values, indicating that all compounds, except C16, possess an optimal permeability and solubility profile and are likely to have good oral bioavailability. Lipinski's 'rule of 5' is widely used for the evaluation of drug-like properties. The obtained results revealed that only two compounds, C1 and C16, violate one of the Lipinski parameters, while all the compounds satisfy the TPSA <140 Å² criterion [94]. Moreover, slightly lower penetration through the blood–brain barrier (BBB) was predicted for the compounds from group A, while group B compounds (especially B3) were assessed to have a higher percentage of unbound drug in plasma compared with the other designed compounds as well as lead molecules. The cytochrome P450 enzymes (CYPs) play an important role in drug metabolism. All compounds were found to be substrates of CYP2D6 and CYP3A4 enzymes and most of them might also be inhibitors. Furthermore, all examined compounds were identified as P-gp substrates. *In silico* toxicity prediction showed that some compounds possess the potential for hERG inhibition and therefore might have an adverse cardiac effect. Compared with clozapine, the designed antagonists possess a lower toxicity risk. The results obtained through this ADMET study may be valuable in further optimization of the compounds regarding their pharmacological effect. Besides, the synthetic difficulty of the designed compounds was evaluated using the SynthDiff score from the ADMET Predictor program (Supplementary Table 12). The score is modeled on the synthetic accessibility score (SA score) and ranges from 0 (simple molecules) to 10 (most difficult for synthesis). The calculation is based on the molecular complexity and fragment contributions [95]. The obtained results revealed that the designed compounds from group A (especially A2) possess the lowest SynthDiff score, while molecules from group B were predicted to have the highest score compared with others. However, it should be taken into account that commercially available fragments were used in the process of rational design of new antagonists, which can significantly facilitate their synthesis.

Based on the obtained findings from 3D-QSAR, molecular docking and ADMET studies, three designed compounds, A2, B3 and C3, were selected as the most promising candidates for further examination, synthesis and *in vitro* testing (Table 5). Following the created computational protocol for rational design, they were predicted to

Table 5. Activity prediction of the most promising candidates for further optimization (A2, B3 and C3) by created 3D-quantitative structure–activity relationship models and experimentally determined activities of lead molecules.

			
	$pK_{i5-HT_{2A}}$	pK_{iD_2}	pK_{iH_1}
A2	9.71	8.82	6.18
B3	9.85	8.06	6.89
C3	10.81	8.16	6.49
ChEMBL90882	8.52	8.60	/
Clozapine	8.04	6.66	8.96
Ziprasidone	10.10	8.30	7.33
Lumateperone	9.27	7.50	/

pKi: Negative logarithm of inhibition constant (-logKi).

have a desired activity and selectivity profile toward 5-HT_{2A}-Rs, D₂-Rs and H₁-Rs as well as favorable drug-like properties compared with lead molecules.

Conclusion

Despite the broad spectrum of currently available drugs for multi-factorial CNS diseases, there is an ongoing need for novel, more effective and safer therapeutics. The current study presented a computational strategy for designing multi-target ligands that simultaneously modulate the activity of 5-HT_{2A}-R and D₂-R, with low affinity for H₁-R. To generate bioactive conformations of ligands for 3D-QSAR modeling, the authors applied MD and molecular docking approaches to these studied targets of interest. Three series of structurally different antagonists were used in 3D-QSAR model building in order to define crucial molecular features, important for high biological activity and selectivity. Based on the findings obtained through the integration of SBDD and LBDD methods, novel 5-HT_{2A}/D₂-R dual antagonists with enhanced activity and a desirable selectivity profile against H₁-R were designed. Accordingly, available fragment libraries were screened in order to identify starting points for the design of high-affinity 5-HT_{2A}/D₂-R antagonists. Afterward, all designed antagonists, along with lead molecules, were used for *in silico* ADMET profiling, in order to analyze and compare their pharmacokinetic properties, as well as synthetic tractability. The most promising candidates, with improved drug-like properties, were selected for further optimization and development of multi-potent drugs, which will be the subject of a future work. All together, the obtained findings may open a new avenue of multi-target drug development and may lead to novel discoveries and greater understanding of dual 5-HT_{2A}/D₂-R antagonists in the treatment of several neuropsychiatric disorders.

Future perspective

Created and statistically validated 3D-QSAR models for 5-HT_{2A}-R, D₂-R and H₁-R present a significant predictive tool, especially in the early stages of the drug discovery process. They could be employed for accurate activity prediction of newly designed analogues that fall within defined applicability domains. Comprehensive pharmacophore analysis may lead to further optimization of molecules with dual antagonistic activity on 5-HT_{2A}/D₂-Rs and lower affinity toward H₁-R, which could be valuable in the development of new therapeutics for the treatment of various neurological diseases and mental disorders. Moreover, selected designed compounds, A2, B3 and C3, will be subjected to further examination, synthesis and *in vitro* testing.

Summary points

- Molecular dynamics simulations, molecular docking and 3D-quantitative structure–activity relationship (3D-QSAR) methods were integrated to perform an extensive pharmacophore analysis of dual 5-HT_{2A}/D₂ receptor (5-HT_{2A}/D₂-R) antagonists with lower affinity toward H₁ receptor (H₁-R).
- The predominant bioactive conformations generated by structure-based drug design methods were used for the calculation of grid independent descriptors and 3D-QSAR model building in order to identify molecular determinants that influence the antagonistic activity of the studied compounds at 5-HT_{2A}-Rs, D₂-Rs and H₁-Rs.
- New dual antagonists with improved activity and selectivity profiles were designed by employing the fragment-based drug design approach. The created 3D-QSAR models were utilized for activity prediction, while molecular docking was used to reveal key interactions of the designed compounds in the binding sites of 5-HT_{2A}-Rs, D₂-Rs and H₁-Rs.
- *In silico* absorption, distribution, metabolism, excretion and toxicity analysis was performed to describe the drug-like properties of new dual antagonists.

Supplementary data

To view the supplementary data that accompany this paper please visit the journal website at: www.future-science.com/doi/suppl/10.4155/fmc-2021-0340

Author contributions

The manuscript was written through the contributions of all authors. All authors have given approval to the final version of the manuscript.

Acknowledgments

The authors acknowledge the Ministry of Science and Technological Development of the Republic of Serbia, Faculty of Pharmacy UB contract no. 451-03-68/2022-14/200161. The authors would like to thank the European Cooperation in Science and Technology (COST) COST Actions CA18133 and CA18240. Numerical simulations were run on the PARADOX-IV supercomputing facility at the Scientific Computing Laboratory, National Center of Excellence for the Study of Complex Systems, Institute of Physics Belgrade, supported in part by the Ministry of Education, Science, and Technological Development of the Republic of Serbia under project no. ON171017.

Financial & competing interests disclosure

The authors have no relevant affiliations or financial involvement with any organization or entity with a financial interest in or financial conflict with the subject matter or materials discussed in the manuscript.

No writing assistance was utilized in the production of this manuscript.

Data sharing statement

The data that support the findings of this study are available from corresponding author M Radan on special request.

References

Papers of special note have been highlighted as: • of interest; •• of considerable interest

1. Collins PY, Patel V, Joestl SS *et al.* Grand challenges in global mental health. *Nature* 475(7354), 27–30 (2011).
2. Ritchie H, Roser M. Mental health. *Our World Data* (2018). <https://ourworldindata.org/mental-health>
3. Trautmann S, Rehm J, Wittchen H. The economic costs of mental disorders. *EMBO Rep.* 17(9), 1245–1249 (2016).
4. Wittchen HU, Jacobi F, Rehm J *et al.* The size and burden of mental disorders and other disorders of the brain in Europe 2010. *Eur. Neuropsychopharmacol.* 21(9), 655–679 (2011).
5. Taquet M, Geddes JR, Husain M, Luciano S, Harrison PJ. 6-month neurological and psychiatric outcomes in 236 379 survivors of COVID-19: a retrospective cohort study using electronic health records. *Lancet Psychiat.* 8(5), 416–427 (2021).
6. OECD/European Union. *Health at a Glance: Europe 2020: State of Health in the EU Cycle*. OECD, Paris, France (2020). www.oecd-ilibrary.org/social-issues-migration-health/health-at-a-glance-europe-2020_82129230-en
7. Frazer A, Hensler JG. Serotonin involvement in physiological function and behavior. In: *Basic Neurochemistry: Molecular, Cellular and Medical Aspects*. Siegel GJ, Agranoff BW, Albers RW (Eds). Lippincott-Raven, PA, USA, 263–292 (1999).
8. Mishra A, Singh S, Shukla S. Physiological and functional basis of dopamine receptors and their role in neurogenesis: possible implication for Parkinson's disease. *J. Exp. Neurosci.* 12, 117906951877982 (2018).

9. Choudhury A, Sahu T, Ramanujam PL *et al.* Neurochemicals, behaviours and psychiatric perspectives of neurological diseases. *Neuropsychiatry (London)* 8(1), 395–424(2018).
- **This work explained the roles of serotonin and dopamine in neurological and mental disorders.**
10. Meltzer H. What's atypical about atypical antipsychotic drugs? *Curr. Opin. Pharmacol.* 4(1), 53–57 (2004).
11. Raote I, Bhattacharya A, Panicker MM. Serotonin 2A (5-HT_{2A}) receptor function: ligand-dependent mechanisms and pathways. In: *Serotonin Receptors in Neurobiology*. Chattopadhyay A (Ed.). CRC Press/Taylor & Francis, FL, USA (2007).
12. Vangveravong S, McElveen E, Taylor M *et al.* Synthesis and characterization of selective dopamine D₂ receptor antagonists. *Bioorg. Med. Chem.* 14(3), 815–825 (2006).
13. Dimatteo V, Pierucci M, Esposito E, Crescimanno G, Benigno A, Digiovanni G. Serotonin modulation of the basal ganglia circuitry: therapeutic implication for Parkinson's disease and other motor disorders. *Prog. Brain Res.* 172, 423–463 (2008).
14. Tsartsalis S, Tournier BB, Gloria Y, Millet P, Ginovart N. Effect of 5-HT_{2A} receptor antagonism on levels of D₂/3 receptor occupancy and adverse behavioral side-effects induced by haloperidol: a SPECT imaging study in the rat. *Transl. Psychiatry* 11(1), 51 (2021).
15. Aringhieri S, Carli M, Kolachalam S *et al.* Molecular targets of atypical antipsychotics: from mechanism of action to clinical differences. *Pharmacol. Ther.* 192, 20–41 (2018).
- **Describes the main mechanism of action of atypical antipsychotics.**
16. Stepnicki P, Kondej M, Koszła O, Żuk J, Kaczor AA. Multi-targeted drug design strategies for the treatment of schizophrenia. *Expert Opin. Drug Discov.* 16(1), 101–114 (2021).
- **A summary of molecular modeling methods in the design of multi-target compounds as well as the advantages and disadvantages of their polypharmacological profile.**
17. Novick D, Montgomery W, Treuer T, Moneta M, Haro J. Real-world effectiveness of antipsychotics for the treatment of negative symptoms in patients with schizophrenia with predominantly negative symptoms. *Pharmacopsychiatry* 50(2), 56–63 (2017).
18. Krause M, Zhu Y, Huhn M *et al.* Antipsychotic drugs for patients with schizophrenia and predominant or prominent negative symptoms: a systematic review and meta-analysis. *Eur. Arch. Psychiatry Clin. Neurosci.* 268(7), 625–639 (2018).
19. Butini S, Nikolic K, Kassel S *et al.* Polypharmacology of dopamine receptor ligands. *Prog. Neurobiol.* 142, 68–103 (2016).
20. Reynolds GP, Kirk SL. Metabolic side effects of antipsychotic drug treatment – pharmacological mechanisms. *Pharmacol. Ther.* 125(1), 169–179 (2010).
- **Confirms the contribution of histamine H₁ receptors in inducing metabolic side effects.**
21. Jafari S, Bouillon ME, Huang XF, Pyne SG, Fernandez-Enright F. Novel olanzapine analogues presenting a reduced H₁ receptor affinity and retained 5HT_{2A}/D₂ binding affinity ratio. *BMC Pharmacol.* 12(1), 8 (2012).
22. Li P, Zhang Q, Robichaud AJ *et al.* Discovery of a tetracyclic quinoxaline derivative as a potent and orally active multifunctional drug candidate for the treatment of neuropsychiatric and neurological disorders. *J. Med. Chem.* 57(6), 2670–2682 (2014).
23. Kore PP, Mutha MM, Antre RV, Oswal RJ, Kshirsagar SS. Computer-aided drug design: an innovative tool for modeling. *Open J. Med. Chem.* 2(4), 139–148 (2012).
24. Leelananda SP, Lindert S. Computational methods in drug discovery. *Beilstein J. Org. Chem.* 12, 2694–2718 (2016).
- **Describes the importance of *in silico* computational methods in the drug discovery process.**
25. Sliwoski G, Kothiwale S, Meiler J, Lowe EW. Computational methods in drug discovery. *Pharmacol. Rev.* 66(1), 334–395 (2014).
26. Verma J, Khedkar V, Coutinho E. 3D-QSAR in drug design – a review. *Curr. Top. Med. Chem.* 10(1), 95–115 (2010).
27. Ferreira L, dos Santos R, Oliva G, Andricopulo A. Molecular docking and structure-based drug design strategies. *Molecules* 20(7), 13384–13421 (2015).
28. Batool M, Ahmad B, Choi S. A structure-based drug discovery paradigm. *Int. J. Mol. Sci.* 20(11), 2783 (2019).
29. Kimura KT, Asada H, Inoue A *et al.* Structures of the 5-HT_{2A} receptor in complex with the antipsychotics risperidone and zotepine. *Nat. Struct. Mol. Biol.* 26(2), 121–128 (2019).
30. Wang S, Che T, Levit A, Shoicher BK, Wacker D, Roth BL. Structure of the D₂ dopamine receptor bound to the atypical antipsychotic drug risperidone. *Nature* 555(7695), 269–273 (2018).
31. Shimamura T, Shiroishi M, Weyand S *et al.* Structure of the human histamine H₁ receptor complex with doxepin. *Nature* 475(7354), 65–70 (2011).
32. Duan X, Zhang M, Zhang X, Wang F, Lei M. Molecular modeling and docking study on dopamine D₂-like and serotonin 5-HT_{2A} receptors. *J. Mol. Graph. Model.* 57, 143–155 (2015).
33. Möller D, Salama I, Kling RC, Hübner H, Gmeiner P. 1,4-Disubstituted aromatic piperazines with high 5-HT_{2A}/D₂ selectivity: quantitative structure-selectivity investigations, docking, synthesis and biological evaluation. *Bioorg. Med. Chem.* 23(18), 6195–6209 (2015).

34. Zhang C, Li Q, Meng L, Ren Y. Design of novel dopamine D₂ and serotonin 5-HT_{2A} receptors dual antagonists toward schizophrenia: an integrated study with QSAR, molecular docking, virtual screening and molecular dynamics simulations. *J. Biomol. Struct. Dyn.* 38(3), 860–885 (2020).
35. Radan M, Ruzic D, Antonijevic M, Djikic T, Nikolic K. *In silico* identification of novel 5-HT_{2A} antagonists supported with ligand- and target-based design methodologies. *J. Biomol. Struct. Dyn.* 39(5), 1819–1837 (2021).
36. Greenwood J, Acharya RB, Marcellus V, Rey JA. Lumateperone: a novel antipsychotic for schizophrenia. *Ann. Pharmacother.* 55(1), 98–104 (2021).
37. Pentacle v 1.07. (2009). <http://www.moldiscovery.com/software/pentacle/>
38. Durán Á, Zamora I, Pastor M. Suitability of GRIND-based principal properties for the description of molecular similarity and ligand-based virtual screening. *J. Chem. Inf. Model.* 49(9), 2129–2138 (2009).
39. Jafari S, Fernandez-Enright F, Huang XF. Structural contributions of antipsychotic drugs to their therapeutic profiles and metabolic side effects. *J. Neurochem.* 120(3), 371–384 (2012).
40. Cooper D, Gupta V. Lumateperone. In: *StatPearls [Internet]*. StatPearls Publishing, FL, USA (2022). www.ncbi.nlm.nih.gov/pubmed/32809679
41. Fernández J, Alonso JM, Andrés JI *et al.* Discovery of new tetracyclic tetrahydrofuran derivatives as potential broad-spectrum psychotropic agents. *J. Med. Chem.* 48(6), 1709–1712 (2005).
42. Phillips ST, de Paulis T, Neergaard JR *et al.* Binding of 5H-dibenzo[a,d]cycloheptene and dibenz[b,f]oxepin analogs of clozapine to dopamine and serotonin receptors. *J. Med. Chem.* 38(4), 708–714 (1995).
43. Graham JM, Coughenour LL, Barr BM, Rock DL, Nikam SS. 1-Aminoindanes as novel motif with potential atypical antipsychotic properties. *Bioorg. Med. Chem. Lett.* 18(2), 489–493 (2008).
44. Lange JHM, Reinders JH, Tolboom JTB, Glennon JC, Coolen HKAC, Kruse CG. Principal component analysis differentiates the receptor binding profiles of three antipsychotic drug candidates from current antipsychotic drugs. *J. Med. Chem.* 50(21), 5103–5108 (2007).
45. Gianotti M, Corti C, Fratte SD *et al.* Novel imidazobenzazepine derivatives as dual H₁/5-HT_{2A} antagonists for the treatment of sleep disorders. *Bioorg. Med. Chem. Lett.* 20(17), 5069–5073 (2010).
46. ChemAxon. MarvinSketch v 16.10.24. www.chemaxon.com/ (2016).
47. Stewart JJP. Optimization of parameters for semiempirical methods. I. Method. *J. Comput. Chem.* 10(2), 209–220 (1989).
48. Stewart JJP. Optimization of parameters for semiempirical methods. II. Applications. *J. Comput. Chem.* 10(2), 221–264 (1989).
49. Roothaan CCJ. New developments in molecular orbital theory. *Rev. Mod. Phys.* 23(2), 69–89 (1951).
50. Frisch MJ, Trucks GW, Schlegel HB *et al.* Gaussian 09. Gaussian, Inc., CT, USA (2009).
51. CambridgeSoft Corporation. Chem3D Ultra v7.0. www.cambridgesoft.com (2001).
52. Berman HM. The Protein Data Bank. *Nucleic Acids Res.* 28(1), 235–242 (2000).
53. Martínez-Rosell G, Giorgino T, De Fabritiis G. PlayMolecule ProteinPrepare: a web application for protein preparation for molecular dynamics simulations. *J. Chem. Inf. Model.* 57(7), 1511–1516 (2017).
54. Morris GM, Huey R, Lindstrom W *et al.* AutoDock4 and AutoDockTools4: automated docking with selective receptor flexibility. *J. Comput. Chem.* 30(16), 2785–2791 (2009).
55. Trott O, Olson AJ. AutoDock Vina: improving the speed and accuracy of docking with a new scoring function, efficient optimization, and multithreading. *J. Comput. Chem.* 31(2), 455–461 (2009).
56. Kaczor AA, Žuk J, Matusiuk D. Comparative molecular field analysis and molecular dynamics studies of the dopamine D₂ receptor antagonists without a protonatable nitrogen atom. *Med. Chem. Res.* 27(4), 1149–1166 (2018).
57. Ranjbar M, Ghafouri H, Salehi F *et al.* Homology modeling, molecular dynamics simulation and cross-docking studies of human histamine-2 (H₂) receptor to obtain a 3D structure for further SBDD studies. *J. Biol. Sci.* 20(1), 22–31 (2019).
58. Feng Z, Alqarni MH, Yang P *et al.* Modeling, molecular dynamics simulation, and mutation validation for structure of cannabinoid receptor 2 based on known crystal structures of GPCRs. *J. Chem. Inf. Model.* 54(9), 2483–2499 (2014).
59. Humphrey W, Dalke A, Schulten K. VMD: visual molecular dynamics. *J. Mol. Graph.* 14(1), 33–38 (1996).
60. Phillips JC, Braun R, Wang W *et al.* Scalable molecular dynamics with NAMD. *J. Comput. Chem.* 26(16), 1781–1802 (2005).
61. Vanommeslaeghe K, Hatcher E, Acharya C *et al.* CHARMM general force field: a force field for drug-like molecules compatible with the CHARMM all-atom additive biological force fields. *J. Comput. Chem.* 31(4), 671–690 (2009).
62. Yu W, He X, Vanommeslaeghe K, MacKerell AD. Extension of the CHARMM general force field to sulfonyl-containing compounds and its utility in biomolecular simulations. *J. Comput. Chem.* 33(31), 2451–2468 (2012).
63. Mitra P, Rastogi A, Rajpoot M, Kumar A, Srivastava V. A QSAR model of olanzapine derivatives as potential inhibitors for 5-HT_{2A} receptor. *Bioinformation* 13(10), 339–342 (2017).

64. Dassault Systèmes BIOVIA. Discovery Studio Visualizer v17.2.0.16349. (2017).
65. Pastor M, Cruciani G, McLay I, Pickett S, Clementi S. Grid-independent descriptors (GRIND): a novel class of alignment-independent three-dimensional molecular descriptors. *J. Med. Chem.* 43(17), 3233–3243 (2000).
66. Durán Á, Pastor M. An advanced tool for computing and handling grid-independent descriptors. *User Man. v1.06.* (2011).
67. Baroni M, Costantino G, Cruciani G, Riganelli D, Valigi R, Clementi S. Generating optimal linear PLS estimations (GOLPE): an advanced chemometric tool for handling 3D-QSAR problems. *Quant. Struct. Relationships* 12(1), 9–20 (1993).
68. Ojha PK, Roy K. Comparative QSARs for antimalarial endochins: importance of descriptor-thinning and noise reduction prior to feature selection. *Chemom. Intell. Lab. Syst.* 109(2), 146–161 (2011).
69. Tropsha A. Best practices for QSAR model development, validation, and exploitation. *Mol. Inform.* 29(6–7), 476–488 (2010).
70. Roy K, Kar S, Das RN. Statistical methods in QSAR/QSPR. In: *A Primer on QSAR/QSPR Modeling*. Springer Cham, Heidelberg, New York, Dordrecht, London, 37–59 (2015).
71. Golbraikh A, Tropsha A. Beware of q²! *J. Mol. Graph. Model.* 20(4), 269–276 (2002).
72. Roy PP, Roy K. On some aspects of variable selection for partial least squares regression models. *QSAR Comb. Sci.* 27(3), 302–313 (2008).
73. Ojha PK, Mitra I, Das RN, Roy K. Further exploring rm2 metrics for validation of QSPR models. *Chemom. Intell. Lab. Syst.* 107(1), 194–205 (2011).
74. OECD. OECD principles for the validation, for regulatory purposes, of (quantitative) structure-activity relationship models. www.oecd.org/chemicalsafety/risk-assessment/37849783.pdf (2004).
75. Roy K, Kar S, Ambure P. On a simple approach for determining applicability domain of QSAR models. *Chemom. Intell. Lab. Syst.* 145, 22–29 (2015).
76. Gramatica P. Principles of QSAR models validation: internal and external. *QSAR Comb. Sci.* 26(5), 694–701 (2007).
77. SPSS, Inc. PASW statistics for Windows, version 18.0. SPSS, Inc., IL, USA (2009).
78. de Souza Neto LR, Moreira-Filho JT, Neves BJ *et al.* *In silico* strategies to support fragment-to-lead optimization in drug discovery. *Front. Chem.* 8, (2020).
- **Highlights the significance of fragment-based drug design in the discovery of new drugs.**
79. Baroni M, Cruciani G, Sciabola S, Perruccio F, Mason JS. A common reference framework for analyzing/comparing proteins and ligands. Fingerprints for ligands and proteins (FLAP): theory and application. *J. Chem. Inf. Model.* 47(2), 279–294 (2007).
80. Cross S, Baroni M, Goracci L, Cruciani G. GRID-based three-dimensional pharmacophores I: FLAP_{pharm}, a novel approach for pharmacophore elucidation. *J. Chem. Inf. Model.* 52(10), 2587–2598 (2012).
81. Cross S, Baroni M, Carosati E, Benedetti P, Clementi S. FLAP: GRID molecular interaction fields in virtual screening. validation using the DUD data set. *J. Chem. Inf. Model.* 50(8), 1442–1450 (2010).
82. van de Waterbeemd H, Gifford E. ADMET *in silico* modelling: towards prediction paradise? *Nat. Rev. Drug Discov.* 2(3), 192–204 (2003).
83. Simulation Plus, Inc. ADMET Predictor 9.5. Simulation Plus, Inc., CA, USA (2019).
84. Nikolic K, Mavridis L, Djikic T *et al.* Drug design for CNS diseases: polypharmacological profiling of compounds using cheminformatics, 3D-QSAR and virtual screening methodologies. *Front. Neurosci.* 10, (2016).
85. Bhattarai A, Wang J, Miao Y. G-protein-coupled receptor–membrane interactions depend on the receptor activation state. *J. Comput. Chem.* 41(5), 460–471 (2020).
86. Aier I, Varadwaj PK, Raj U. Structural insights into conformational stability of both wild-type and mutant EZH2 receptor. *Sci. Rep.* 6(1), 34984 (2016).
87. Chikalov I, Yao P, Moshkov M, Latombe JC. Learning probabilistic models of hydrogen bond stability from molecular dynamics simulation trajectories. *BMC Bioinformatics* 12(Suppl. 1), S34 (2011).
88. Zhang D, Lazim R. Application of conventional molecular dynamics simulation in evaluating the stability of apomyoglobin in urea solution. *Sci. Rep.* 7(1), 44651 (2017).
89. Jain AN. Bias, reporting, and sharing: computational evaluations of docking methods. *J. Comput. Aided Mol. Des.* 22(3–4), 201–212 (2008).
90. Shi L, Javitch JA. The binding site of aminergic G protein-coupled receptors: the transmembrane segments and second extracellular loop. *Annu. Rev. Pharmacol. Toxicol.* 42(1), 437–467 (2002).
91. Im D, Inoue A, Fujiwara T *et al.* Structure of the dopamine D2 receptor in complex with the antipsychotic drug spiperone. *Nat. Commun.* 11(1), 6442 (2020).
92. Munk C, Isberg V, Mordalski S *et al.* GPCRdb: the G protein-coupled receptor database – an introduction. *Br. J. Pharmacol.* 173(14), 2195–2207 (2016).

93. Snyder GL, Vanover KE, Zhu H *et al.* Functional profile of a novel modulator of serotonin, dopamine, and glutamate neurotransmission. *Psychopharmacology (Berl.)* 232(3), 605–621 (2015).
94. Ritzén A, David L. Physicochemical parameters of recently approved oral drugs. In: *Successful Drug Discovery*. Fischer J, Klein C, Childers W (Ed.). Wiley-VCH, Weinheim, Germany, 35–53 (2019).
95. Ertl P, Schuffenhauer A. Estimation of synthetic accessibility score of drug-like molecules based on molecular complexity and fragment contributions. *J. Cheminform.* 1(1), 8 (2009).